# Doctorate Dissertation

# 博士論文

## Development of an Assay Method for Evaluating Cell Fusion Events Using Split Luciferase Reconstitution Techniques

## （スプリットルシフェラーゼ再構成技術を用いた細胞融合評価法の開発）

**A Dissertation Submitted for Degree of Doctor of Philosophy**
**July 2017**

**平成 29 年 7 月博士（理学）申請**

**Department of Chemistry, Graduate School of Science,**
**The University of Tokyo**

**東京大学大学院理学系研究科化学専攻**

**LI Qiao-jing**

**李　喬婧**

# Abstracts

Myogenesis-promoting chemicals are an important source of new pharmaceuticals for treatment of skeletal muscle atrophy that impairs quality of life. Thus, a high-throughput method that can screening such compounds rapidly and robustly is required. However, previous methods for evaluating the myogenesis-promotion are based either on microscopic imaging or fluorescence determination, which are labor-intensive and time-consuming or may be interfered by constitutive fluorescence of the sample compounds. So, there has not been a method that is ideal for high-throughput screening of myogenesis-promoting compounds. Therefore, the purpose of this study is to develop a bioluminescence-based method which does not require microscopic imaging, by using protein *trans*-splicing-based split luciferase reconstitution technique. (**Chapter 1**)

To develop the method, a pair of split firefly luciferase (Fluc) probes were designed: the amino-terminal fragment of firefly luciferase (Fluc) fused with the N-termini of a naturally split DnaE intein (N-probe) and the carboxyl-terminal fragments of Fluc fused with the C-termini of split DnaE intein (C-probe). The two probes were then introduced into C2C12 cells respectively to develop two myoblast cell lines (N-cell and C-cell) and the mixture of the two cells were used to assess the effects of chemical compounds on myogenesis. It was confirmed in advance that cell fusion between the two cells during myogenesis enables the reconstitution of Fluc from the two probes, and the reconstitution relies on the split DnaE inteins that spontaneously and covalently connect the two split Fluc fragments. Furthermore, the luminescence intensity produced by the reconstituted Flucs was shown to be linearly correlated to

the frequency of cell fusion during myogenesis, and sufficiently sensitive to reflect the myogenesis-promoting effect of IGF-1 on a 96-well microtiter plate scale. An assay based on a 96-well microtiter plate was then established using this method system, and the robustness of the assay for screening compounds having a myogenesis-promoting effect comparable to IGF-1 was verified. (**Chapter 2**)

The 96-well microtiter plate-based assay was applied to a high-throughput screening of myogenesis-promoting compounds in 1,191 pharmacologically proven bioactive small molecules (Prestwick Chemical). As a result, two hits compounds, Imatinib and Doxazosin mesylate, were obtained. In addition, dose-dependent effects of Imatinib and Doxazosin mesylate on myogenesis of C2C12 cells were investigated by the present assay as well as the conventional evaluation of fusion index. Two results were consistent that the optimum concentration for promoting the myogenesis of C2C12 cells was ascertained to be 6.0 μmol $L^{-1}$ for Imatinib and 4.0 μmol $L^{-1}$ for Doxazosin mesylate, respectively. Prominent features of the present myogenesis-assay system are robustness and rapidity. In case of our 96-well plate assay, robust luminescence signals were acquired within 1 s from individual wells. Such rapidity in data-acquisition allows the present system to be applicable to high-throughput screening of chemical compounds. (**Chapter 3**)

In conclusion, the present myogenesis assay system provides a promising approach for identification of myogenesis-promoting compounds through a robust high-throughput screening. And it may be useful for basic myogenesis studies, tissue engineering and drug discovery in addition to broad applications to assess cell fusion events of different kinds for cell lines and organelles.

# Table of contents

## Abbreviation

| | |
|---|---|
| DMEM | Dulbecco's Modified Eagle Medium |
| C-cell | The C2C12 cell harboring the C-probe |
| cDNA | Complementary deoxyribonucleic acid |
| CFNKSH | Cysteine-Phenylalanine-Asparagine-Lysine-Serine-Histidine |
| C-probe | Fusion protein of DnaEc and FlucC |
| DMSO | Dimethyl sulfoxide |
| DNA | Deoxyribonucleic acid |
| DnaEc | The carboxyl-terminal fragment of DnaE |
| DnaEn | The amino-terminal fragment of DnaE |
| EDTA | Ethylenediaminetetraacetic acid |
| Em | Emission wavelength |
| Ex | Excitation wavelength |
| FBS | Fetal bovine serum |
| Fluc | Firefly luciferase |
| FlucC | The carboxyl-terminal fragment of Fluc |
| FlucN | The amino-terminal fragment of Fluc |
| GFP | Green fluorescent protein |
| GPA | β-guanidinopropionic acid |
| GS | Glycine-Serine |
| HCl | Hydrochloric acid |
| HEPES | 4-(2-hydroxyethyl)-1-piperazineethanesulfonic acid |
| HRP | Horseradish peroxidase |
| IGF-1 | Insulin-like growth factor 1 |
| IgG | Immunoglobulin G |
| IRES | Internal ribosome entry site |
| MAPK | Mitogen-activated protein kinase |
| MHC | Myosin heavy chain |
| N-cell | The C2C12 cell harboring the N-probe |
| N-probe | Fusion protein of FlucN and DnaEn |

| | |
|---|---|
| PBS | Phosphate buffer saline |
| Puro | Puromycin |
| RNA | Ribonucleic acid |
| SD | Standard deviation |
| SDS | Sodium dodecyl sulfate |
| SDS-PAGE | Sodium dodecyl sulfate polyacrylamide gel electrophoresis |
| TNFα | Tumor necrosis factor alpha |
| Tris | Tris(hydroxymethyl)aminomethane |

# Chapter 1

# General introduction

## 1-1. Demand for high-throughput screening methods for compounds that promote muscle formation

Skeletal muscles are the largest metabolic organs of human body, which are responsible for voluntary movements of the body and production of heat for maintaining body temperature. [1] Skeletal muscle is comprised of multiple bundles of muscle fibers. And the muscle fibers are multinucleated muscle cells, also called myocytes. Between the basement membrane and the cell membrane of muscle fibers, there are multipotent cells called satellite cells.[2] **(Fig. 1-1)** In adult body, the satellite cells are normally mitotically quiescent but they can be activated to regenerate skeletal muscle in response to stress that is induced by weight bearing or trauma, to repair the muscle tissue.[3] However, it is still inevitable for skeletal muscle wasting to occur under poor rehabilitations due to aging, diseases and serious injuries.[4] Therefore, drugs that promote skeletal muscle regeneration are in demand for saving the quality of human life when skeletal muscle wasting occur. In order to find candidates of such drugs from existing chemical libraries, a robust and high-throughput screening method is required for evaluating myogenesis promotion.

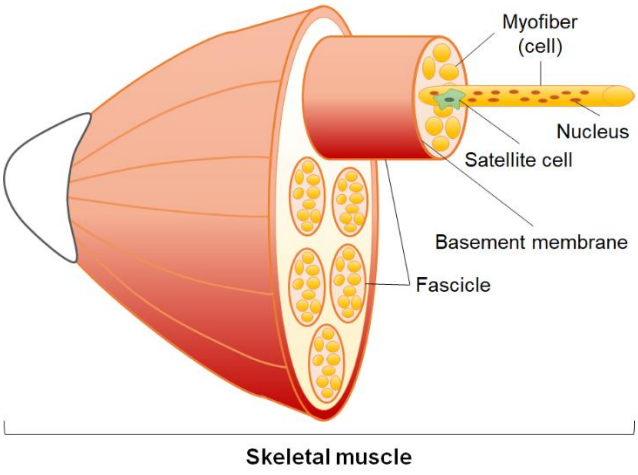


**Fig.1-1. The structure of a skeletal muscle.**

## 1-2. Myogenesis and myocyte fusion

The process that satellite cells forming skeletal muscles is called myogenesis. Myogenesis is a successive process involving cell differentiation and cell fusion. **(Fig. 1-2)** It begins with the activation of satellite cells to re-enter the cell cycle, giving rise to proliferative progeny cells called myoblasts.[5] After several cycles of proliferation, the proliferating myoblasts terminally differentiate to myocytes that can be characterized by the expression of myogenin,[6] and then the mononucleated myocytes fuse together to form multinucleated myotubes, which further mature into myofibers, successively. In myotubes and myofibers, major structural myofibrillar proteins such as myosin heavy chain (MHC) are expressed.[7] In the process of myogenesis, the myocyte fusion is a key step in producing functional skeletal muscle.

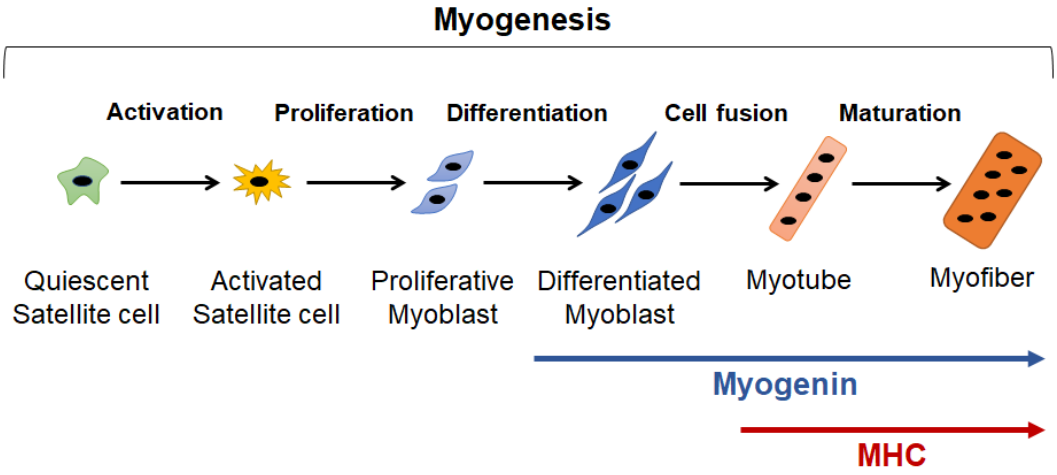


**Fig. 1-2. The myogenesis process and the marker proteins for each step.**

## 1-3. Previous methods for evaluating myogenesis

### 1-3-1. Microscopic imaging-based analyses of myotube formation

Previously, the extent of myogenesis were mostly evaluated through the physical size (diameter and area) of myotubes/myofibers and the frequency of cell fusion.[8,9] And fusion index was the most commonly used parameter for evaluating the frequency of myocytes fusion.[10,11] The fusion index refers to the ratio of the number of nuclei in the myotubes/myofibers to the total number of nuclei, therefore it is equivalent to the cell fusion rate in the case of cell fusions among mononucleated cells without involving fusion of nuclei. As described in **Section 1-2**, the primary satellite cell has a single nucleus, which remains independent after cell fusion. The fusion index is therefore directly proportion to the frequency of myocyte fusion during myogenesis, thus it can be used reliably to estimate the extent of myogenesis, theoretically. However, for counting the number of nuclei inside and outside the myotubes/myofibers to measure the fusion index, it is inevitably required to obtain an immunofluorescence image of one cell culture from which the nuclei and myotubes/myofibers are distinguishable. However, it is a labor-intensive procedure to obtain the immunofluorescence images and calculate the number of nuclei, thus measurement of fusion index is time-consuming **(Fig. 1-3)**. In addition, the image can only cover part of the whole cell culture, thus, multiple images of different areas are essential for a sample. And measurement of fusion index is also susceptible to operator bias as it is often difficult to determine whether a nucleus is inside or outside a myotube. With all of these aspects in mind, it is clear that the fusion index is not a suitable indicator for high-throughput determination.

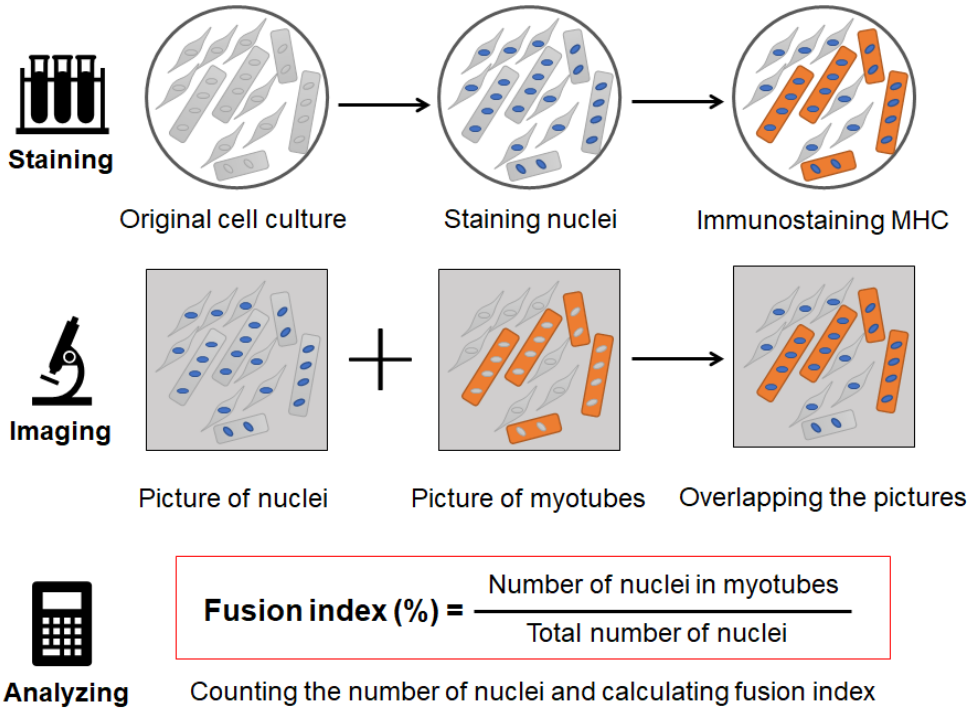


**Fig. 1-3. Procedure of measuring fusion index for myogenetic cell samples.**

To simplify the evaluation of myogenesis, Velica and Bunce developed a simple method to quantify myotube formation using micrographs of Jenner–Giemsa stained C2C12 cultures.[12] In the method, the extent of myotube formation correlates with the increase in pixels within the darkest tones that resulted by Jenner–Giemsa dyes staining myotubes. Based on the image histogram obtained from the photograph, the sum of the darkest shades was measured to represent the myotube density. And these analyses were done by using a ImageJ software. Unlike artificially counting the number of nuclei inside and outside the myotube in the case of fusion index measurement, the software-based analysis is unbiased. However, the method still cannot get rid of the process of microscopic imaging, which is an obstacle to achieving high-throughputs.

### 1-3-2. Fluorescence analyses of myotube formation without using microscope

The method proposed by Miyake and McDermott, that identifies myotubes through staining their robust mitochondrial network using MitoTracker, a mitochondrial fluorescent tracking dye, requires no microscopic imaging since the fluorescent signal intensity increases as the muscle differentiation progresses, which can be simply digitized by measuring the fluorescence intensity. In addition, the method does not require fixed cell sample.[13] The authors mentioned the possibility of using this method to screen chemicals, genomes, etc., that affect muscle regeneration or maintenance in a high-throughput manner, but have not really tried it.

There is also another fluorescence-based approach proposed by Kodaka and Hata, in which the split-GFP complementation technique is used for assessing the frequency of cell fusion during myogenesis.[14,15] In this method, the fluorescence intensity was also shown to correlate with the progression of myotube formation, but data for high-throughput screening has not yet been provided.

The simple fluorescence-based analyses that correlate the extent of myogenesis with fluorescence intensity overcame the shortcoming of the methods relying on microscopic imaging. However, considering constitutive fluorescence properties of many chemical compounds, a fluorescence-based assay is not ideal for chemical compound screening.

Consequently, although microscopy-based and fluorescence-based analyses have contributed to investigation of myogenesis, both have respective disadvantages, thus a new non-fluorescence-based method without microscopic-imaging is required for a high-throughput screening of myogenesis-promoting compounds.

## 1-4. Purpose of this study

The key points summarized for the above-mentioned backgrounds are as follows: the healthiness of skeletal muscles is essential for keeping human lives in a high quality, however skeletal muscle wasting is inevitable in the cases of aging, diseases and injurie, thus, development of new drugs to treat such muscle wasting requires a robust and quantitative screening method that detects myogenesis. As myocytes fusion is a consequential step of myogenesis, thus the extent of myogenesis can be compared via the frequency of myocytes fusion. However, the methods previously used to determine the frequency of cell fusion are based on either microscopic imaging or fluorescence analysis, that are labor intensive or may be interfered by the constitutive fluorescence property of the sample chemicals. Therefore, the purpose of this study is to develop an efficient method that is suitable for a high-throughput screening of myogenesis-promoting compounds, and it will be a novel bioluminescence-based myogenesis assay, which requires no microscopic imaging and can assess the extent of myogenesis on 96-well microtiter plates scale. In the development of such method, the protein *trans*-splicing-based split luciferase complementation technique was adopted. The technical principle involved in this study are described in the following sections.

### 1-5. Strategy of the luminescence-based cell fusion assay

The bioluminescence-based myogenesis system **(Fig. 1-4)** comprises a pair of probe proteins, which consist of complementary split luciferase fragments and split intein parts. In the case of no barrier between a pair of probes, the two probes interact to reconstitute a complete luciferase, which can emit luminescence signal. The spontaneous interaction is mediated by the split intein parts, which successively induce a protein *trans*-splicing reaction, linking the complementary luciferase fragments covalently. Thus, luciferases are stably reconstituted.

To evaluate the cell fusion during myogenesis with the probes, the two types of probes were separately introduced to the sample cell, so that they were kept separated through cell membranes before cell fusion occurring. And when the cell fusion occurred between the cells harboring different probes, the luminescence signal will be produced as above mentioned. Theoretically speaking, the frequency of the cell fusion and the corresponding luminescent signal will increase with the promotion of myogenesis, so the luminescence intensity can be used as an indicator for assessing the prograss of myogenesis.

In this study, firefly luciferase (Fluc) and a naturally split DnaE intein from the cyanobacterium *Synechocystis* sp. PCC6803 (DnaEn and DnaEc) were used to construct the probes.

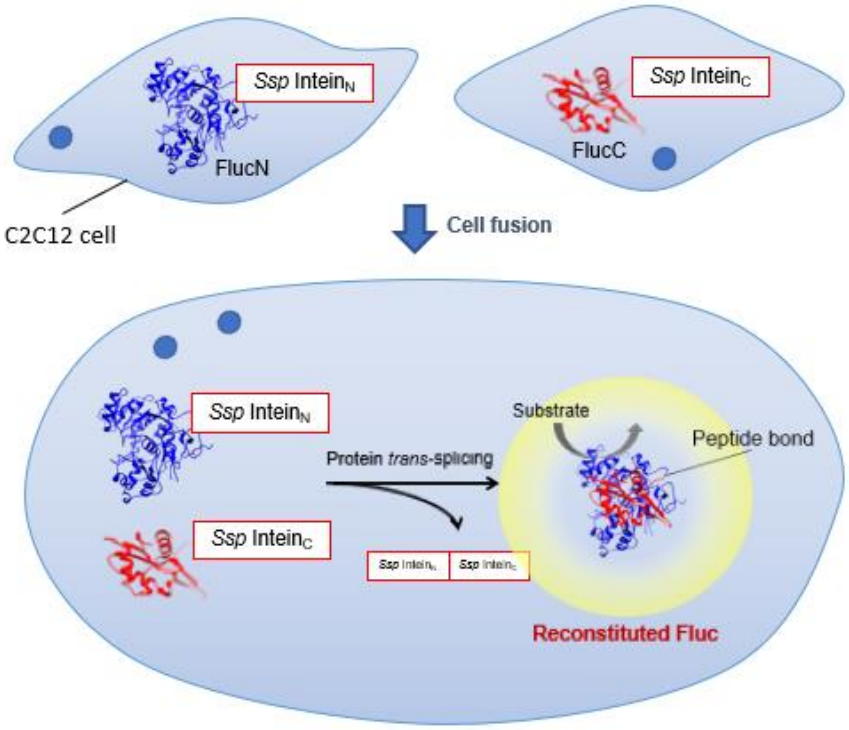


**Fig. 1-4. Scheme of the bioluminescence-based analysis of cell fusion.**

## 1-6. Techniques involved in developing the assay method

### 1-6-1. Bioluminescence analysis with firefly luciferase

Bioluminescence is the emission of light in living organisms resulting from an enzymatic reaction catalyzed by proteins called luciferase. Among the bioluminescence systems, the firefly luciferin–luciferase system is most widely studied and applied to bioluminescence-based assays.[16,17]

In the firefly luciferin–luciferase system, Fluc is an enzyme protein that playing the role of a catalyzer, and luciferin is the substrate, which reacts with adenosine triphosphate (ATP) in the presence of an oxygen molecule and $Mg^{2+}$ under the catalyzation of Fluc. The reaction produces the first singlet excited state of electron in oxyluciferin, which immediately transfers to its ground state, producing light radiation in the visible region of the spectrum (540–600 nm). Details of the luminescent reaction were shown in **Fig. 1-5**.

Fluc has been successfully used in different in vitro and in vivo systems[18,19] as a reporter molecule because of the following advantages:

(1) The quantum yield of the bioluminescent Fluc reaction is extremely high (>88%), which could facilitate the signal detection at both cellular and tissue levels.[20]

(2) The Fluc substrate, D-luciferin, is very stable, can remain in culture medium over days.[21]

(3) D-luciferin can penetrate the cell membrane without relying on the P-glycoproteins.[22]

(4) No cytotoxicity induced by either firefly luciferase overexpression or D-luciferin treatment has been reported in recent studies.[19]

(5) Unlike the fluorescence analysis, no light excitation was required for the light-

emitting reaction, wherefore the luciferase-based bioluminescent analysis gives a very low background signal and causes much fewer cell damages.[23]

(6) Luciferase is a kind of protein, that can be genetically encoded and expressed *in situ*. Thus, there is no need for the luciferase to be delivered to the imaging target like other organic fluorescent agents or inorganic nanoparticles. Furthermore, the luciferase can be modified to the protein of interest easily via genetic engineering.[24]

In a word, luminescent reaction by Fluc is very simple, harmless and require no external light source or cofactors, giving wide applications in bioanalysis.

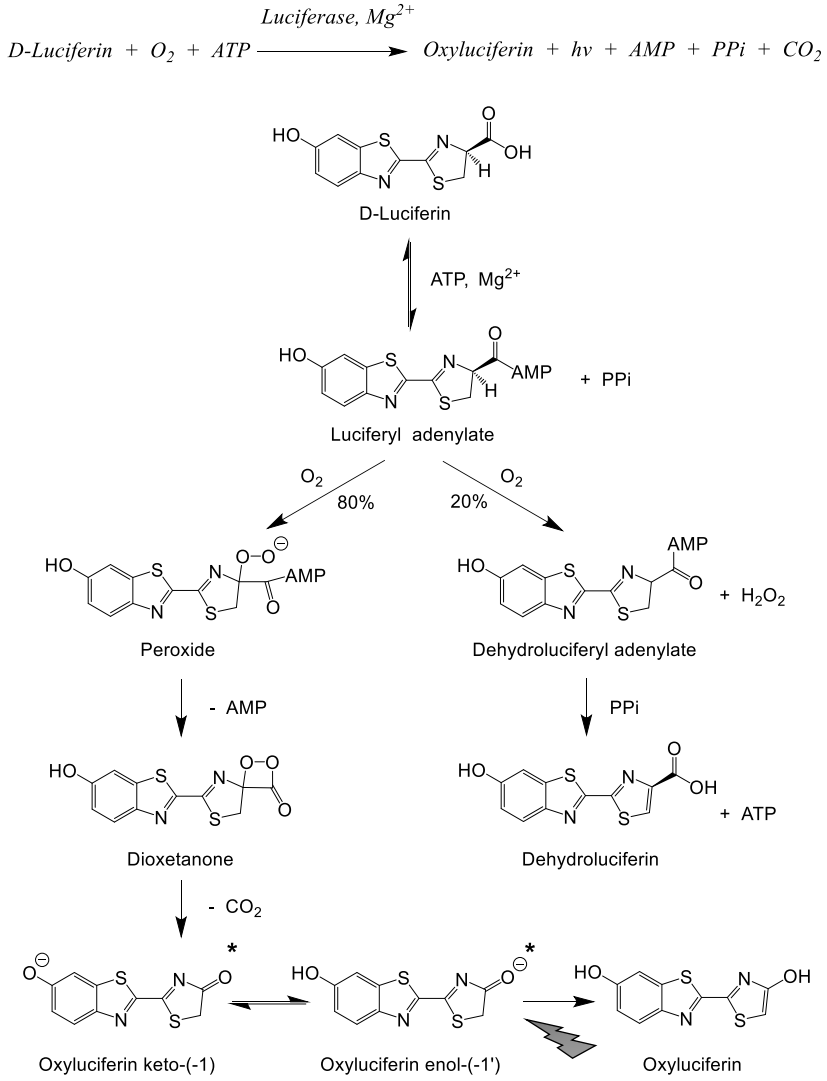


**Fig. 1-5. Bioluminescence reaction of D-Luciferin catalyzed by Fluc.** Luciferyl adenylate is formed from D-luciferin, firstly. Around 80% of adenylate is then oxidized via a single electron-transfer mechanism into peroxide. The peroxide further transforms and leads to production of oxyluciferin and emission of light. Oxyluciferin is initially formed in a neutral form and then loses a proton via the excited state proton transferring to give keto-(−1) or enol-(−1′), which are thought to be the actual light emitters inside the luciferase pocket. The remaining 20% adenylate forms hydrogen peroxide and dehydroluciferin.

### 1-6-2. Split luciferase complementation analysis

Luciferase can be used not only in its intact form but also in a split form for bioluminescence analysis.[25,26] Although luciferase split into two fragments at several specific sites loses the catalytic ability, the catalytic ability can be regained in the case that a complementation occurs between the two split fragments when they are brought into close proximity. In the case of Fluc, such complementation can occur when Fluc was split at the following amino acid sites: 398 [27], 415 [28], 416 [29,27], 437 [30,31], 445 [30], 455 [30].

The complementation of split luciferases is rapid and reversible.[32] And the split luciferase complementation assay has suitable dynamic range and high signal-to-noise ratio. [33]

In the case of split Fluc, the complementation cannot occur spontaneously and requires an external force to bring the two fragments to a proximity. This feature made split Fluc complementation a powerful tool for the detection of protein–protein interactions both in vivo and in vitro. In these studies, two split fragments, the amino-terminal and carboxyl-terminal fragments of Fluc (FlucN and FlucC), were respectively fused to the target proteins to be assessed for the interaction between them. If the two target proteins interacted with each other, bring the FlucN and FlucC into close proximity, the FlucN and FlucC complementated to reconstitute a complete firefly luciferase, producing a luminescence signal. **(Fig. 1-6A)** Otherwise, if the protein pair does not interact or dissociate, the luciferase activity will cease accordingly. Therefore, split Fluc complementation assay allows the assessment of protein interaction with high signal-to-background ratios and reversibility. In addition, the high signal-to-background property also made split Fluc fragments to be excellent

signal molecules for a molecular probe. In these cases, FlucN and FlucC were separately connected to the recognizing molecule (e.g. recaptor, scFv) to form the probe against detecting target.[34,35] **(Fig. 1-6B)** And along with the target recognition, probes are aggregated, prompting luciferase reconstitution and subsequent generation of luminescence.

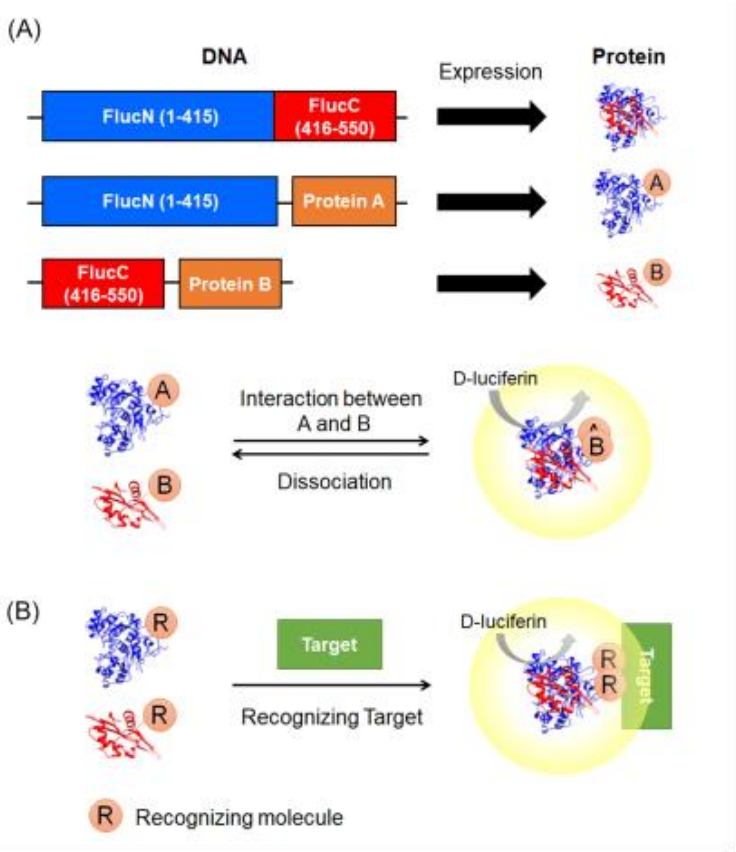


**Fig. 1-6. Application of split Fluc complementation analysis.** (A) Split Fluc complementation applied for detecting protein-protein interaction; (B) Split Fluc complementation used as signal molecule of a molecular probe. If "R" is a protein, a Fluc fragment can be fused to "R" by genetic engineering; if "R" is a non-protein compound, the purified luciferase fragment can be linked to "R" by an *in vitro* chemical reaction.

### 1-7. Protein *trans*-splicing-based split luciferase complementation

As be mentioned above, reversibility is one advantage of split luciferase complementation analysis at the aspect of observing protein-protein interaction. However, in some cases, the complementary stability of luciferase rather than reversibility is required. Thus, protein *trans*-splicing-based split luciferase complementation technique [31,36] emerged.

In 1990, when the mature protein sequence of the yeast vacuolar ATPase (Vma1) and its corresponding mRNA were compared, researchers surprisingly found that the mature protein had a lower molecular weight than expected from the encoding sequence. This phenomena indicated that one part of the protein had lost after translation.[37,38] The lost part of protein, which excised themselves and joined the remaining portions (the exteins) of protein precursors together, was named Intein. And the process of this posttranslational modification that analog to intron splicing on RNA level, was named protein splicing. In *trans*-splicing inteins, the intein is split into two (or perhaps more) domains, which are then divided into N-termini and C-termini. And exteins were connected via the N-termini and C-termini by the following protein *trans*-splicing reactions **(Fig. 1-7)** [39]:

(1) N-Intein and C-Intein first assemble together to form a dimer like structure with a newly formed catalytic core next to the exteins.

(2) The tertiary structure of the intein, once correctly formed, facilitates an N→O/S acyl rearrangement of Cystein/Serine at its N-terminal serine or cysteine residue. The result is an ester or thioester bond, respectively between the side-chain and the peptide backbone of the N-extein.

(3) The two exteins are then linked by trans(thio)esterification involving the N-

terminal serine or cysteine residue of the C-extein. The C-terminus of the N-extein is now covalently bound to the N-terminal side-chain of the C-extein, while its backbone still retains its normal peptide bond to the intein.

(4) The C-terminal asparagine of the intein undergoes self-cyclisation to form a succinimidyl moiety. The peptide bond between the intein and the extein is thereby broken, resolving the branched intermediate.

(5) In a final reaction, an O/S→N acyl shift results in the two exteins now being linked by an amide bond, indistinguishable from a ribosome-assembled fusion protein.

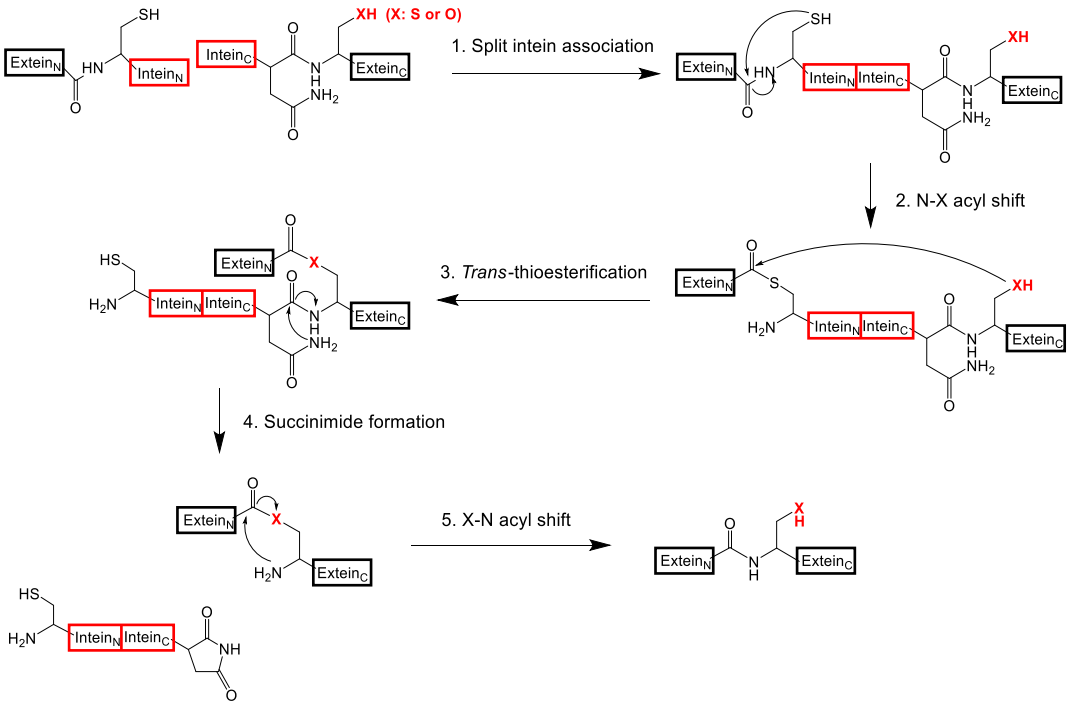


**Fig. 1-7. Canonical mechanism of protein *trans*-splicing reaction by split inteins.**

Therefore, by fusing the amino- and carboxyl-terminal fragments of a luciferase respectively to the N-termini and C-termini of a split intein, the luciferase fragments can be connected like the exteins via the protein *trans*-splicing reaction. In addition, the interaction between the split inteins occurs spontaneously and does not require forces from the outside. Thus, a complete luciferase can be reconstituted spontaneously and stably through the protein *trans*-splicing-based split luciferase complementation.

## 1-8. In vitro model of myogenesis: C2C12 cell line

The C2C12 is an immortal line of mouse skeletal myoblasts, originally established from satellite cells of the thigh muscle of a two-month-old C3H mouse 70 hours after a crush injury.[40] The C2C12 cells can differentiate rapidly, produce extensive contracting myotubes expressing characteristic muscle proteins, thus is a widely used model to study myogenesis and cell differentiation *in vitro*.[41,42]

When undifferentiated, the wild-type C2C12 cells are flat, fusiform or star-shaped mononucleated cells having a radial branching morphology consisting of long fibers extending in many directions.[43] After induced differentiation, they become elongated, and as the progress of differentiation, cell fusion proceeds and myotubes elongate to become protein-rich structures that express myosin, α-actin, troponin, and other components of the muscle-contractile machinery.[44] Myosin and actin appear much more concentrated in the myotubes than in mononuclear cells.[43]

The induction of differentiation of C2C12 cells can be easily achieved by shifting the pre-confluent C2C12 cultures from high-serum (10% fetal bovine serum) to low-serum conditions (2–5% horse serum), which induces cell cycle exit, commitment to myogenic differentiation, and fusion between myoblasts to form multinucleated myotubes.[45] Besides, apoptosis has been widely described in differentiating systems where it seems to balance the cell proliferation in the process of maturity. [46,47,48,49]

## 1-9. Contents of the study

To offer an efficient method for a high-throughput screening of myogenesis-promoting compounds, the new bioluminescent myogenesis assay was developed by utilizing the protein *trans*-splicing-based split luciferase complementation technique in the following procedures.

Firstly, two cell lines respectively harboring one of the pair of probes were prepared based on the C2C12 cell, and they were evaluated from abilities of myotube formation and differentiation, the separate expression of one of the probes and production of luminescence accompany with the cell fusion.

Secondly, using the two cells, the method was established according to the strategy described above (see **Section 1-5**), and evaluated in applicability of the detecting cell fusion and identifying promotion of the cell fusion by chemical compounds. A 96-well plate-based assay was then developed and validated for its robustness and quality in high-throughput screening of myogenesis-promoting compounds.

Finally, by using the 96-well plate-based assay, the screening of myogenesis-promoting compounds was conducted among 1,191 pharmacologically-proven bioactive molecules (Prestwick Chemical), already used as medicines and relevant mechanisms of efficacies were clear.

# Chapter 2

# Development of the 96 well plate-based high-throughput cell fusion quantitative assay

## 2-1. Introduction

To rescue the quality of human life threatened by muscle wasting, a new myogenesis assay, which was suitable for a high-throughput screening of myogenesis-promoting compounds, is in demand. Because the previous methods for assessing the myogenesis progression were either requiring imaging by microscope or based on fluorescence determination, herein, the bioluminescence-based myogenesis assay was developed. Since the key step in myogenesis to generate functional skeletal muscles is the myocyte fusion, in this method, the production of luminescence is related to myocyte fusion. In order to develop the method, a pair of genetically encoded probes was designed according to the protein *trans*-splicing-based split luciferase reconstitution technique. C2C12 myoblast cells expressing either of the probes were prepared and cultured in the same cultivation dishes. Fusion of the cells that occurs in the myogenesis process produces the encounter of the probes to each other in the cytoplasm, and then the cell fusion was detected from the luminescence of reconstituted Fluc which generated via protein *trans*-splicing reactions. The assay system was constituted and evaluated for its performance in high-throughput screening of myogenensis-promoting compounds on 96-well plates.

## 2-2. Materials and Methods

### 2-2-1. Materials

The C2C12 cell was purchased from ATCC (Manassas, VA). A DNA polymerase (PrimeSTAR), restriction enzymes and Western Blot Blocking Buffer (Fish Gelatin) were purchased from Takara Bio Inc. (Kusatsu, Shiga, Japan). Dulbecco's modified Eagle's medium [DMEM (4.5 g $L^{-1}$ glucose) with L-glutamine and HEPES and without sodium pyruvate] and 0.5 g $L^{-1}$ Trypsin/0.53 mmol $L^{-1}$ EDTA Solution were purchased from Nacalai Tesque Inc. (Kyoto, Japan). Platinum-A retroviral packing cells and pMXs-IRES-Puro retroviral expression vector were obtained from Cell Biolabs, Inc. (San Diego, CA). Fetal bovine serum (FBS) and Mouse anti-β-actin antibody [AC-15] were purchased from Sigma-Aldrich Corp. (Saint Louis, MO). Penicillin-Streptomycin, horse serum and phenol-red free DMEM were purchased from Gibco BRL (Rockville, MD). Puromycin, blasticidin and mouse anti-V5 antibody were obtained from Invitrogen Corp. (Carlsbad, CA). TransIT-LT1 transfection reagent was purchased from Mirus Bio LLC (Madison, WI). D-Luciferin potassium salt was obtained from Wako Pure Chemical Industries Ltd (Osaka, Japan). Nitrocellulose blotting membrane with 0.45 μm pore size and horseradish peroxidase (HRP) - conjugated anti-mouse or anti-rabbit IgG were obtained from GE Healthcare (Buckinghamshire, England). Rabbit anti-Fluc antibody was obtained from Abcam (Cambridge, U.K.). Mouse anti-Myc antibody was obtained from Cell Signaling Technology Inc. (Danvers, MA). Mouse anti-myogenin [F5D] antibody was obtained from Santa Cruz Bio Inc. (Dallas, TX). SuperSignal West Femto Maximum Sensitivity Substrate and an anti-mouse IgG labeled with Alexa Fluor 568 were purchased from Thermo Fisher Scientific Inc. (Waltham, MA). Hoechst 33342 was purchased from

Molecular Probes Inc. (Eugene, OR). Mouse anti-Myosin Heavy Chain (MHC) [MF20] antibody was obtained from R&D Systems (Minneapolis, MN). FluorSave reagent was purchased from EMD Millipore (Burlington, MA). KOD-Plus-mutagenesis kit was purchased from TOYOBO (Osaka, Japan).

### 2-2-2. Plasmids construction

An *E. coli* strain, DH5α, was used as the bacterial host for the construction of all plasmids. Based on the cDNA of Fluc, DnaEn and DnaEc, the following DNA fragments were prepared from the original cDNA by PCR: (1) BamHI-Kozak consensus sequence (gccacc)-FlucN (1–415 aa)-KpnI; (2) KpnI-FlucC (416-550 aa)-Myc-Stop codon-EcoRI; (3) KpnI-GS-DnaEn-V5-Stop codon-EcoRI; (4) BamHI-Kozak-DnaEc-CFNKSH-KpnI. The fragments 1 and 3, 4 and 2 were connected at the KpnI restriction enzyme site, and the generated two DNA fragments were inserted into pMXs-IRES-Puro retroviral expression vector at the restriction enzyme sites BamHI and EcoRI. As a result, pFlucN-DnaEn-V5 and pDnaEc-FlucC-Myc were constructed. pFlucN-V5 and pFlucC-Myc were constructed from pFlucN-DnaEn-V5 and pDnaEc-FlucC-Myc by removing the DnaEn and DnaEc with the KOD-Plus-mutagenesis kit.

### 2-2-3. Cell culture

Platinum-A retroviral packing cells were maintained in DMEM (4.5 g $L^{-1}$ glucose) supplemented with 10% FBS, 100 unit $mL^{-1}$ penicillin, 100 μg $mL^{-1}$ streptomycin, 1 μg $mL^{-1}$ puromycin and 10 μg $mL^{-1}$ blasticidin. The C2C12 cells were cultured in DMEM supplemented with 10% FBS, 100 unit $mL^{-1}$ penicillin and 100 μg $mL^{-1}$ streptomycin. The N-cells and C-cells were cultured in DMEM supplemented with 10%

FBS, 100 unit $mL^{-1}$ penicillin, 100 μg $mL^{-1}$ streptomycin and 2.5 μg $mL^{-1}$ puromycin (proliferation medium).

**2-2-4. Preparation of retrovirus vectors**

The retrovirus containing the RNA of the N-probe was prepared by transfecting the retroviral expression vector, pFlucN-DnaEn-V5, into Platinum-A cells using the TransIT-LT1 transfection reagent according to the manufacture's protocol (the ratio of plasmid of N-probe to TransIT-LT1 reagent adopted was 1:3), culturing the cells for 48 h, and collecting the supernatants of the cell culture which contain the retroviruses. The supernatants were used immediately or aliquoted for storage at -30°C until use. For preparation of the retrovirus containing the RNA of C-probe, the same procedure was performed by using pDnaEc- FlucC-Myc.

**2-2-5. Preparation of the N-cells and C-cells**

The C2C12 cells was seeded to a 10-cm dish at $1.5\times 10^5$ cells per dish in the proliferation medium which removed streptomycin and puromycin. After 1 day of culturing, the cell cultures were added with 0.5 mL of the above-mentioned retrovirus supernatant for the N-probe or the C-probe to introduce and integrate the gene of the probes to the genome of the cells. The cells were subcultured in the proliferation medium, which contains 2.5 μg $mL^{-1}$ puromycin, for 3 passages, and the survived cells were used as the N-cells or C-cells, which were stored in liquid nitrogen until use. The cells less than 10 passages after resuscitation from the frozen cell stock were used in all experiment.

### 2-2-6. Differentiation

Cells were seeded to a 3.5-cm dish at $4.0 \times 10^5$ cells per dish or a well of a 96-well plate at $1.4 \times 10^4$ cells per well. The cells were cultured for two days to reach full confluence and washed with 1 mL of phosphate buffer saline (PBS) once. And then, a differentiation medium, which substituted the 10% FBS in the proliferation medium with 1% horse serum, was added to the cell culture to induce the differentiation of the myoblasts. The differentiation medium was changed every two days.

### 2-2-7. Observation with a phase-contrast microscope

The phase-contrast images of the cells were obtained under a CKX31N-11PHP phase-contrast microscope (Olympus Corp., Tokyo, Japan) with a UPlanFLN 4x objective lens (Olympus Corp.) by using a XZ-2 digital camera (Olympus Corp.) mounted an NY-XZ1 microscope adapter (Olympus Corp.).

### 2-2-8. Western blot analysis

Cells cultured to a full confluence in a 3.5-cm dish were collected and lysed in 120 μL lysis buffer (1% SDS, 10% glycerol, 10% 2-mercaptoethanol, 0.001% Bromophenol Blue, 50 mmol $L^{-1}$ Tris/HCl, pH 6.8). Samples of 20 μL lysates were subjected to SDS-PAGE using 15% SDS polyacrylamide gels and were transferred onto a nitrocellulose blotting membrane with 0.45 μm pore size. A polyclonal anti-Fluc antibody was used to detect the fragments of Fluc. An anti-V5 antibody was used for detecting the V5-tag on the N-probe, an anti-Myc antibody was adopted to detect the Myc-tag on the C-probe and the reconstituted Fluc, an anti-myogenin [F5D] antibody was employed to detect the myogenin, and an anti-β-actin [AC-15] antibody was used for the detection

of β-actin as a control sample. Then, the primary antibodies were labeled by using an HRP-conjugated anti-mouse or anti-rabbit IgG. The HRP activities were visualized by using the SuperSignal West Femto Maximum Sensitivity Substrate with an image analyzer (LAS-3000 plus; Fuji Film Co., Tokyo, Japan).

**2-2-9. Immunofluorescence**

The cells were seeded on a piece of cover slip which was in a 3.5-cm dish at $4.0 \times 10^5$ cells per dish to conduct the differentiation. The cell culture sample on the cover slip was firstly stained with Hoechst 33342 (1:1000 dilution of 1 mg $mL^{-1}$ stock in water) at 37°C for 20 min for visualization of nuclei. Then, the sample was fixed with 4% paraformaldehyde in PBS at 37 °C for 30 min and washed with PBS. Next, the sample were permeabilized with 0.2% Triton X-100 in PBS at room temperature (25 °C) for 5 min and then blocked with 0.2% Gelatin (blocking solution) from cold water fish skin in PBS for 1 h at room temperature (25 °C) or overnight at 4 °C. The blocked sample was incubated with an anti-MHC antibody and an anti-mouse IgG labeled with Alexa Fluor 568, successively. The cover slip with the cell sample was mounted by using FluorSave reagent on a slide glass and fluorescence images (Ex/Em: 405 nm / 455 nm for Hoechst 33342 and Ex/Em: 559 nm / 572 nm for myotubes) were obtained at four areas (n=4) with a UPLSAPO 60X objective lens (Olympus Corp.) by using a confocal fluorescent microscope (IX-81, FV-1000D; Olympus Corp., Tokyo, Japan).

**2-2-10. Measurement of luminescence intensity**

Substrate solution for the luminescence measurement was prepared by adding D-luciferin into a phenol red-free DMEM. The medium of the cell samples was replaced

by 2.0 mL and 100 μL of the substrate solution for a 3.5-cm dish and a 96-well plate-based measurement, respectively. A luminescence intensity was measured by Luminometer (Kronos Dio AB-2550; ATTO Technology Inc., Amherst, NY) or a microplate multimode reader (TriStar LB 941; Berthold Technologies GmbH & Co. KG, Bad Wildbad, Germany), correspondingly.

### 2-2-11. Calculation of fusion index

From the above-mentioned immunofluorescence imaging data, the total number of nuclei and the number of nuclei inside myotubes (MHC positive area) were counted. And the fusion index was calculated via the following equation:

$$\text{Fusion index} = \frac{Number\ of\ the\ nuclei\ inside\ myotubes}{Total\ number\ of\ nuclei}$$

### 2-2-12. The 96-well plate-based assay for myogenesis-promoting compounds

The N-cells and C-cells was mixed at 1:1 (n/n) homogeneously and seeded to a white opaque 96-well plate at $1.4 \times 10^4$ cells per well. The cells were cultured for two days to reach full confluence and washed by using 200 μL of PBS once. And then, to induce the differentiation of the cells and test the chemical samples, 200 μL of differentiation medium or the above-mentioned compound-containing medium was added to each well, successively. After 4 days of differentiation, the medium was replaced by 100 μL of PBS to washout the chemical sample once, and then the measurement of luminescence intensities was conducted well-by-well immediately for 1 s per well. The measurement was repeated five times for 10 min, until the luminescence intensities

reached plateaus. The average of the five measurements was calculated as the luminescence intensity corresponding to the chemical sample.

## 2-3. Results and discussion

### 2-3-1. Design of the myogenesis assay system

In the development of the present myogenesis-assay system, two genetically encoded probes based on a protein trans-splicing and split luciferase reconstitution techniques were designed. The pair of probe proteins consists of split Fluc fragments and a naturally split DnaE intein from the cyanobacterium *Synechocystis* sp. PCC6803.[50] The split DnaE inteins comprise amino-terminal 123 amino acids (DnaEn) and carboxyl-terminal 36 amino acids (DnaEc). Some of their complexes possess an ability to ligate the N-exteins and C-exteins.[51] The Fluc was split at the position between 415 and 416 amino acids to produce amino-terminal and carboxyl-terminal fragments, namely, FlucN and FlucC, respectively.[28] The FlucN was fused to the amino terminus of the DnaEn (designated as N-probe), whereas the FlucC was fused to the carboxyl terminus of the DnaEc (designated as C-probe) **(Fig 2-1A)**. Then, two stable cell lines that express either N-probe or C-probe were established by using a C2C12 myoblast cell line[43] (N-cell and C-cell, respectively). The cell fusion between the N-cells and C-cells allows the N-probes to encounter the C-probes in the cytoplasm, where a protein trans-splicing reaction occurs between DnaEn and DnaEc. As a result, FlucN fuses with FlucC via a peptide bond between the serine (S) and cysteine (C)[52] to form reconstituted Fluc **(Fig 2-1B)**.

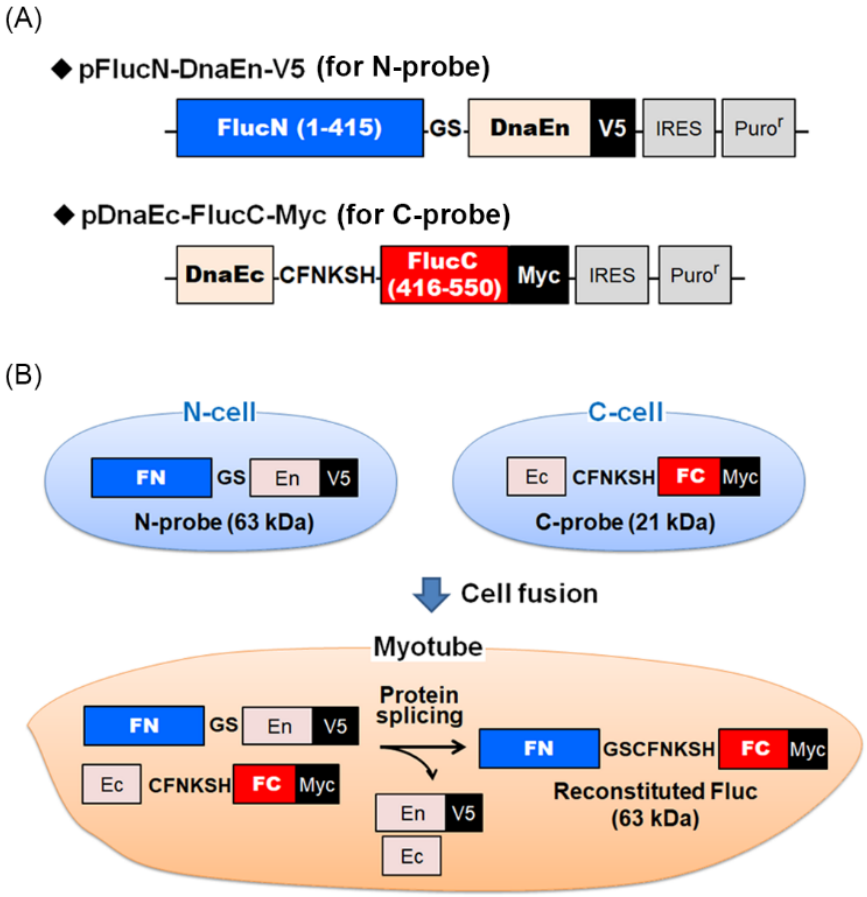


**Fig. 2-1. Design of the myogenesis assay system.** (A) The schematic of the retroviral expression vectors for the N-probe and C-probe. The vectors also include puromycin resistance gene. (B) The principle for monitoring the cell fusion. The abbreviations are defined in the main text except FN, FC, En and Ec that respectively indicate FlucN, FlucC, DnaEn and DnaEc here only in this figure.

### 2-3-2. Differentiation of C2C12 cells

The investigation was conducted whether the C2C12 cells could differentiate and form myotubes. The C2C12 cells were spread to a 3.5 cm-dish in the proliferation medium (10% FBS) and cultured to full confluent. And then the medium was changed to the differentiation medium (2% Horse serum) and this was recorded as Day 0. Afterwards, the morphological change of the cells was observed under a phase-contrast microscope every two day. As a result, a bipolar spindle shape appeared on Day 2, which is a typical feature of differentiated C2C12 cells. And some tubular-structured small myotubes were observed subsequently on day 4, which finally grew longer passing day 6. **(Fig. 2-2)**. Therefore, the C2C12 cell can differentiate well, and was used for the following experiments.

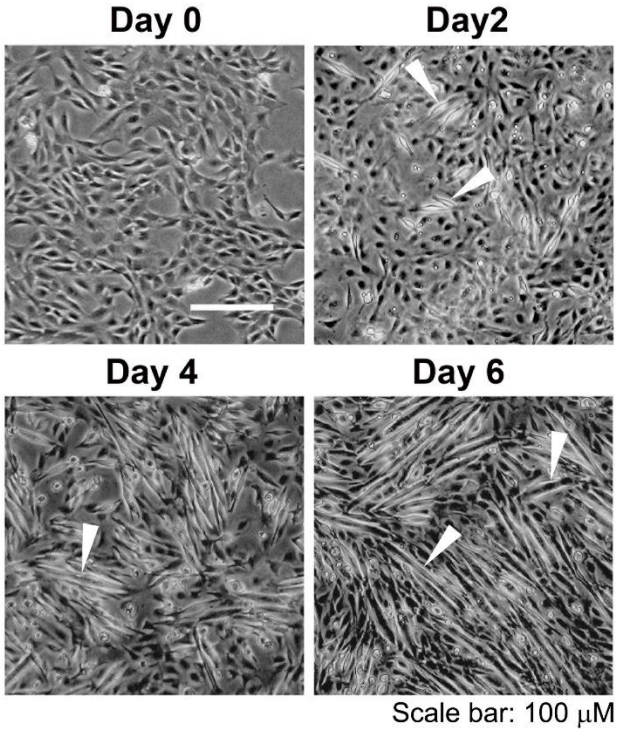


**Fig. 2-2. Myotubes formation in the C2C12 cells on various differentiation days (Days 0, 2, 4, and 6).** Some of the myocytes and myotubes were indicated by white arrows.

### 2-3-3. Confirmation of probe reconstitution via split intein in C2C12 Cells induced

Herein, it was investigated whether the N- probe and C-probe can reconstitute a luciferase, which can generate the luminescence signal, and the split intein fragments are requisites for the reconstitution. The genes of the N-probe, C-probe, FlucN (DnaEn were removed from N-probe) and FlucC (DnaEc were removed from C-probe) were introduced into C2C12 cells in varying combinations through retroviral infection. In the case where the components were introduced in pairs, an equal volume of retrovirus solution for each component was used. And the total volume of retrovirus used for infection was consistent among the test groups except for the intact C2C12 cell control. After infection, the cells were cultured to full confluence in 3.5-cm dishes and then the luminescence signals were determined for each dish by adding 2 mL of D-luciferin (1.0 mmol $L^{-1}$) and counting the signal for 30 s. To further confirm the successful infection of each component, the cell cultures were applied to western blot to determine the components via the corresponding V5-tag or Myc-tag. As a result, luminescence signals were detected only from the cells introduced with N-probe and C-probe together, whereas detectable luminescence was not observed from the cells introduced with neither N-probe, C-probe, FlucN and FlucC alone, or the pairs of N-probe with FlucC and C-probe with FlucN **(Fig. 2-3)**, and the C-probe and FlucC were not detectable by western blot. Considering the degradation of the C-probe and FlucC, we treated the cell culture by MG-132 (20 μmol $L^{-1}$, 4 hours), which is a widely used proteasome inhibitor, to inhibit the protein degradation.[53,54,55] After MG-132 treatments, both the C-probe and FlucC became detectable by western blot. Thus, the retroviral infection was successful, and the expression of each components occurred

in the C2C12 cells, but the C-probe and FlucC expressed were not stable and easily degraded. However, the reconstitution accompanied the luminescence emission occurred when the N-probe and C-probe existed in the cytosol of C2C12 cells at the same, indicating that the C-probe was once expressed fully before the degradation and it could be stabilized if met the N-probe before the degradation. In addition, it was also confirmed that both of two split DnaE fragments were required for the reconstitution.

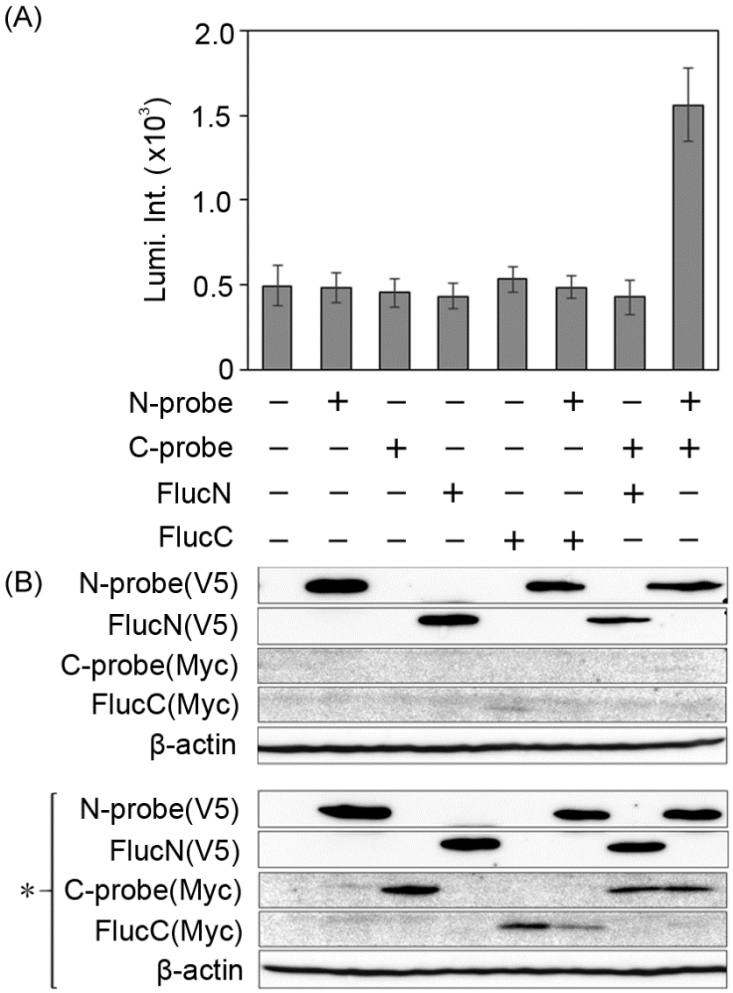


**Fig. 2-3. Confirmation of reconstituting Fluc from the N-probe and C-probe via the split intein.** (A)The luminescence intensities (Mean±SD, *n*=3) generated by the C2C12 cells being introduced N-probe, C-probe, FlucN and FlucC in varying combinations. The genes of each components were introduced into C2C12 cells by retroviral infection. 1.0 mmol $L^{-1}$ D-luciferin were added and the luminescence signal was counted for 30 s. (B) Western blot analysis of the components expressed in each group via the corresponding V5-tag or Myc-tag. * The sample treated by MG-132 (20 μmol $L^{-1}$, 4 hours).

### 2-3-4. Characterization of the N-cell and C-cell

The N-cell and C-cell were developed by respectively introducing the N-probe (N-cell) and C-probe (C-cell) into the C2C12 cell, and was evaluated from the aspects of the ability in forming myotubes, the expression of the corresponding probe and the luminescence production before and after the cell differentiation.

#### 2-3-4-1. Myotube formation in the mixture of N-cell and C-cell

Firstly, to see whether myotubes can be formed in the N-cells, C-cells and their mixture, the morphological changes of cells in the cell cultures of the N-cells, C-cells and their cell mixture were observed under the phase-contrast microscope, respctively. From the imaging of the cell cultures just before (Day 0) and 6 days after the induction of differentiation (Day 6), myotube formation was observed in both N-cells and C-cells, and in their mixture as well, on Day 6 but not on Day 0. **(Fig. 2-4)** The results suggest that the N-cells and C-cells were undifferentiated initially but were differentiated and fused into myotubes after the induction of differentiation. And, myotubes were formed in the similar level in the N-cells and the C-cells by visual inspection. Therefore, the N-cells and C-cells have myoblast properties applicable for myogenesis assessment.

The time-dependent differentiation was also confirmed via the expression levels of a myocyte marker, myogenin,[6] for the mixture of N-cells and C-cells after the induction of differentiation. The cell mixture of the N-cells and C-cells was seeded to 3.5-cm dishes, cultured to full confluence and induced differentiation (Day 0). The cells were collected day by day from Day 0 to Day 7 and analyzed by Western blotting. The results show a time-dependent myogenin expression pattern, namely, its expression appeared at 2 days after myogenesis initiation (Day 2) and increased over time to reach the maximum value on Day 5. **(Fig. 2-5)**

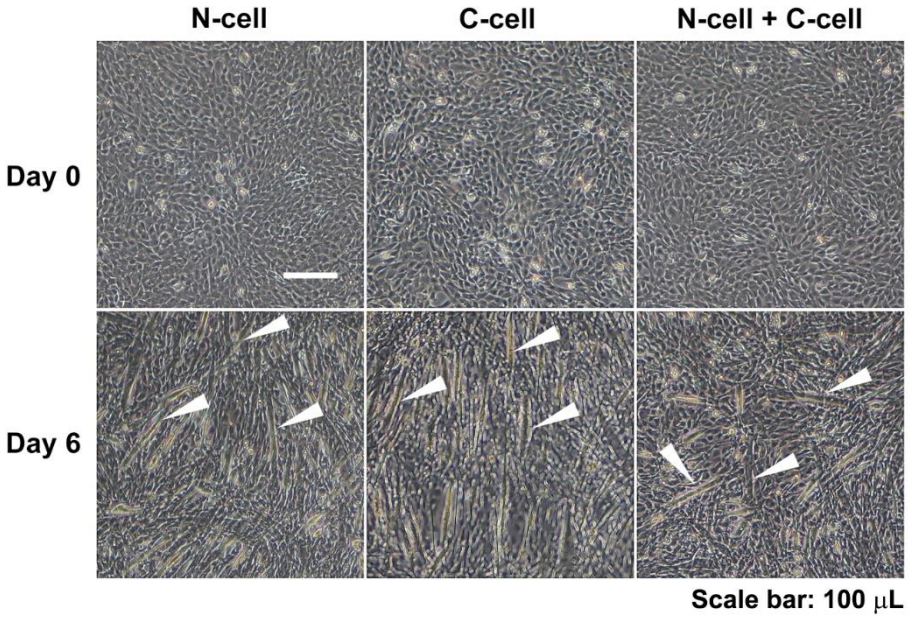


**Fig. 2-4. Myotube formation in the cell culture of N-cell, C-cell and their mixture.** Some of the myotubes were indicated by white arrows**.**

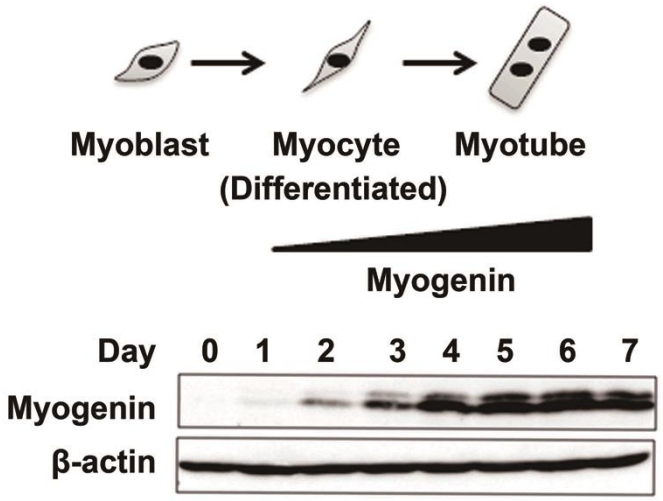


**Fig. 2-5. Western blot analysis of myogenin expression in the mixture of N-cells and C-cells after induction of differentiation.** β-actin was determined as a reference for the amounts of the proteins in electrophoresis.

### 2-3-4-2. Expression of N-probe and C-probe in N-cell and C-cell

Next, to confirm that the N-probe was expressed in the N-cell alone while the C-probe was expressed in the C-cell alone, the N-cells, C-cells and their mixture on varying days of differentiation (Days 0, 2, 4, 6, and 8) were tested by western blot, respectively, for the expression of N-probe and C-probe. The N-probe (V5) and C-probe (Myc) were detected via V5-tag and Myc-tag, respectively, and detected directly by an anti-Fluc polyclonal antibody. As a result, the N-probes were expressed stably in the N-cells and the N-C cell mixture. And the reconstituted Fluc (Myc) was also observed in the mixed samples from Day 4. However, the C-probe was not detected in C-cells alone, even though it was detected in the mixture of N-cells and C-cells on Day 4-8. **(Fig. 2-6)** Because the phenomenon of the C-probe degradation in the C2C12 cells was indicated from the previous results **(Fig. 2-3)**, to reconfirm the previous conclusion, I conducted the treatment for the C-cells with MG-132. As a result, the C-probe became detectable and increased over time of the treatment **(Fig. 2-7)**, again suggesting that the C-probes were degraded by proteasome degradation pathway when the probe existed alone in the C2C12 cells (C-cells), whereas the C-probe was stabilized through the interaction with the N-probe when the N-cell fused to the C-cell.

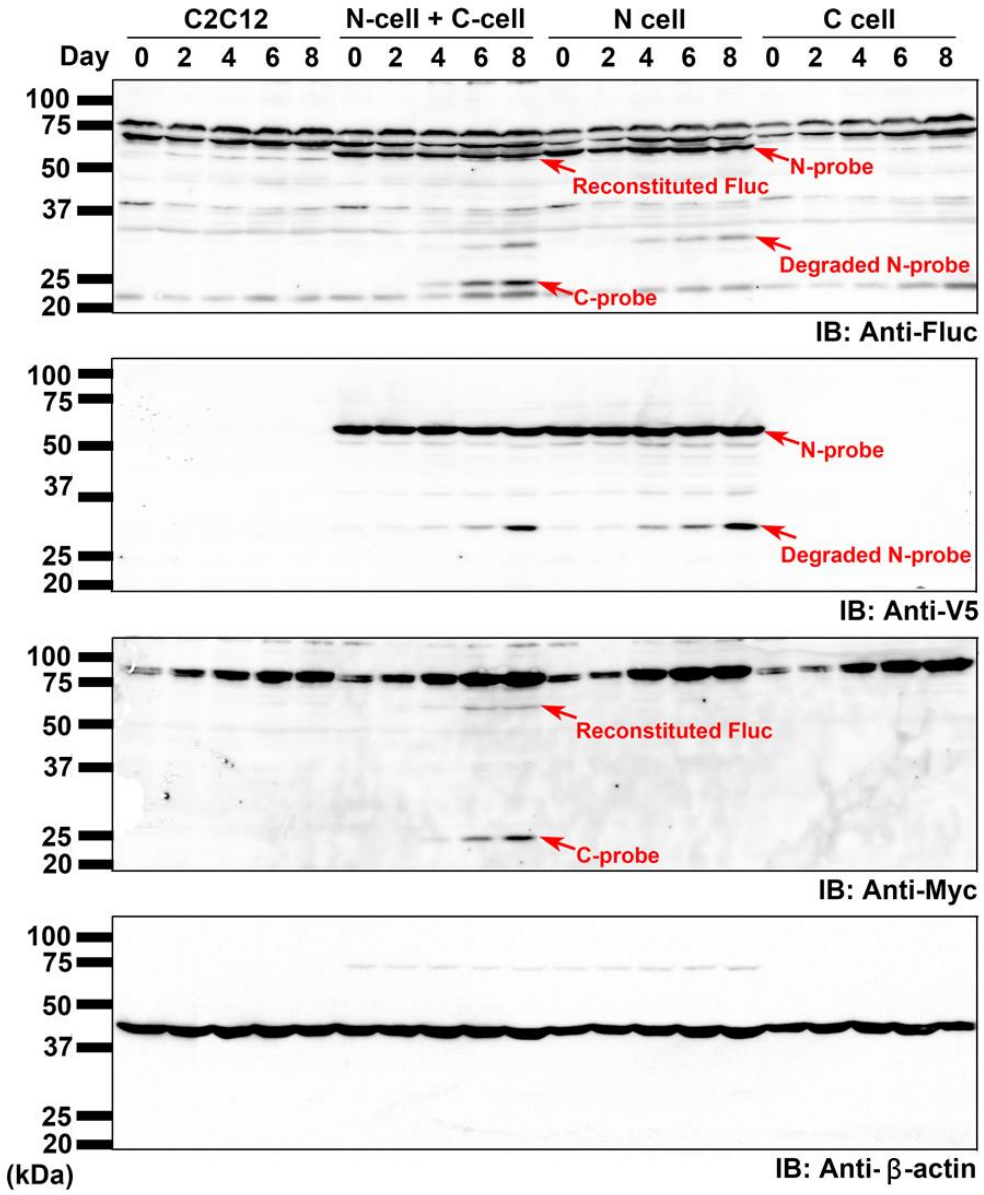


**Fig. 2-6. Western blotting analysis of the expression of N-probe and C-probe, and the reconstitution of Fluc in the N-cell, the C-cell and the N-C cell mixture during differentiation.** The intact C2C12 cells were tested as negative control. The N-probe (63 kDa), the C-probe (21 kDa), the reconstituted Fluc (63 kDa) and the degraded N-probe were indicated by red arrows. β-actin was blotted as a reference for the amounts of the proteins in electrophoresis.

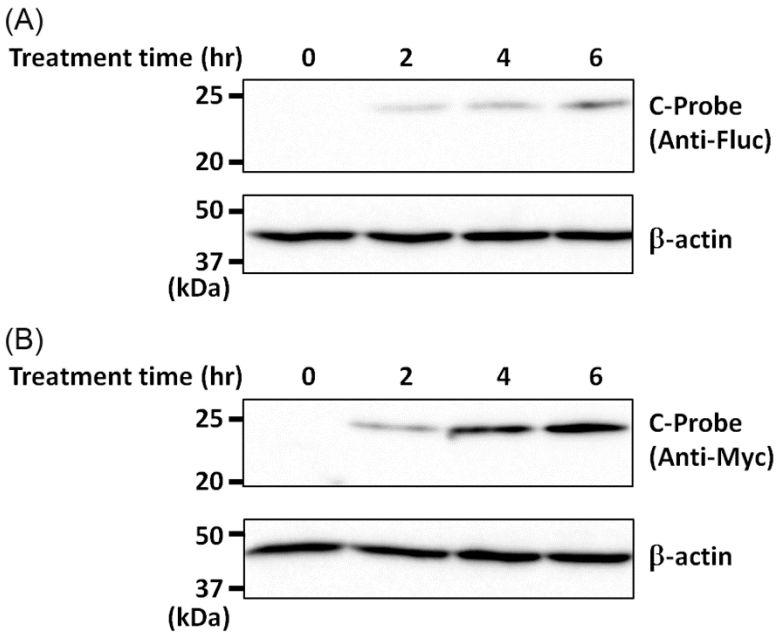


**Fig. 2-7. C-probes detected from the C-cells before and after being treated by MG-132.** MG-132 were added to the culture medium at 20 μmol $L^{-1}$ and the treatment time were 0, 2, 4 and 6 hours, respectively. The C-probe was blotted with anti-Fluc antibody (A) and anti-Myc antibody (B), respectively. β-actin was blotted as a reference for the amounts of the proteins in electrophoresis.

**2-3-4-3. Production of luminescence before and after cell differentiation by N-cell, C-cell and their mixture**

Finally, the luminescence produced by the N-cell, C-cell and their mixture before and after the differentiation were measured. The N-cell and C-cell were cultivated in 3.5-cm dishes separately or as a 1:1 (n/n) mixture, and differentiated for 6 days. Luminescence intensities were determined for the cell cultures before and after differentiation. The results manifest that the luminescence signal was not detectable from the N-cells and C-cells neither before or after the differentiation, or from the mixture of N-cells and C-cells before the differentiation. And the obvious luminescence signal was obtained from the N-C cell mixture after the differentiation. **(Fig2-8)** The result of luminescence test is consistent with that of the western blotting which suggested that a Fluc was reconstituted only after differentiation. **(Fig. 2-6)**

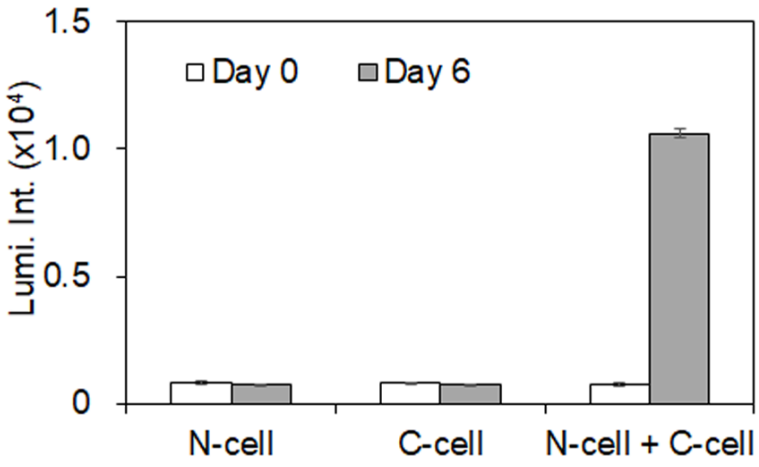


**Fig. 2-8. Luminescence intensities (± SD, n = 3) produced from N-cell, C-cell and their mixture before (Day 0) and after differentiation (Day 6).** 1 mmol $L^{-1}$ D-luciferin was added and the luminescence intensities were counted for 30 s.

### 2-3-5. Correlation of luminescence intensity with differentiation and cell fusion

To evaluate myogenesis extent, the luminescence signal generated from the mixture of N-cells and C-cells should correlate with the frequency of the cell fusion. Therefore, the correlation between the luminescence intensity and the cell fusion frequency was investigated. The 1:1 (n/n) mixture of N-cells and C-cells differentiated for 0, 2, 4 and 6 days were measured for the luminescence intensity and imaged by the immunofluorescence, from which the fusion indexes were further calculated. The immunofluorescence imaging results show an obvious increase in the cell fusion as the myotubes became bigger **(Fig. 2-9A)**. Correspondingly, the fusion indexes calculated based on the imaging data also presented an increasing trend from Day 0 to Day 6 **(Fig. 2-9B)**. When the luminescence intensity was shown against the fusion index according to the differentiation days, the luminescence intensity showed a linear correlation with the fusion index **(Fig. 2-9C)**. The results indicated that the N-cell and C-cell can be used as an indicator of the cell fusion in myogenesis and the method has comparable performance of the fusion index.

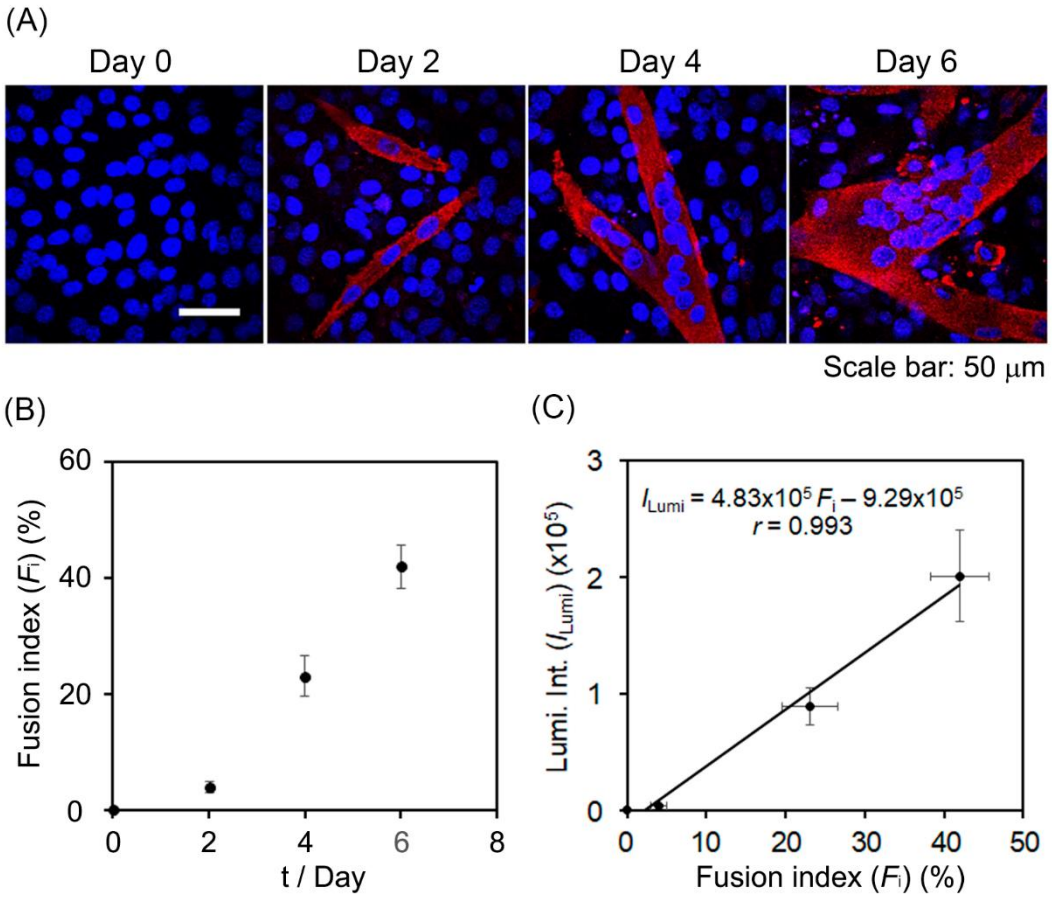


**Fig. 2-9. Correlation between luminescence intensities and cell fusion frequency.** (A) Immunofluorescence analysis of the mixture of N-cells and C-cells on varying differentiation days. The nuclei (blue dots) were stained with Hoechst 33342; myotubes (red) were labeled with anti-MHC antibody; (B) Fusion index (± SD, n = 3) calculated from the immunofluorescence images on varying differentiation days. (C) Correlation between the luminescence intensity (± SD, n = 3) and the fusion index (± SD, n = 3) 1 mmol $L^{-1}$ D-luciferin was added and luminescence intensities were counted for 30 s.

### 2-3-6. The 96-well plate-based assay using the N-cell and C-cell for evaluating myogenesis-promotion by chemical compounds

To assess the applicability of the present system for examining the drug efficacy in myogenesis induction in the 96-well plate, progressions of the cell fusion upon treatment with myogenesis promoters, β-guanidinopropionic acid (GPA, 1.0 mmol $L^{-1}$)[56,57] and the insulin-like growth factor 1 (IGF-1, 10 ng $mL^{-1}$)[58,59] and an inhibitor, tumor necrosis factor alpha (TNFα, 20 ng $mL^{-1}$)[60,61] were assessed. In advance, the promotion and inhibition of the myogenesis created by the chemicals were confirmed on the intact C2C12 cells. The chemicals were contained in the differentiation medium during all the differentiation process, and the myotube formation in cell cultures were observed on Day 0, Day 4 and Day 6 **(Fig. 2-10A)**. The imaging data show that the myotube formation was prompted by GPA and IGF-1 while it was inhibited by TNFα as expected. And then, the mixture of N-cells and C-cells were cultivated on the 96-well plate to induce the differentiation in the presence of each chemicals, respectively, and the luminescence intensity was detected well by well for 1 s per well. As a result, the decrease/increase in luminescence intensities for the TNFα, the IGF-1, and the GPA groups were consistent with the effects of these agents **(Fig. 2-10B)**. Therefore, the possibility of evaluating chemical effects on myogenesis quantitatively by using this system to the 96-well plate-based assay can be inferred. To minimize time consuming and maximize the throughput of the assay, the days of differentiation was set to 4 days and the luminescence signal was counted for merely 1 second for each well by the 96-well plate reader. Under such conditions, although the absolute level of luciferase signals was not significant, it was practical for identifying the differences caused by compounds on the cell fusion in a high-throughput manner.

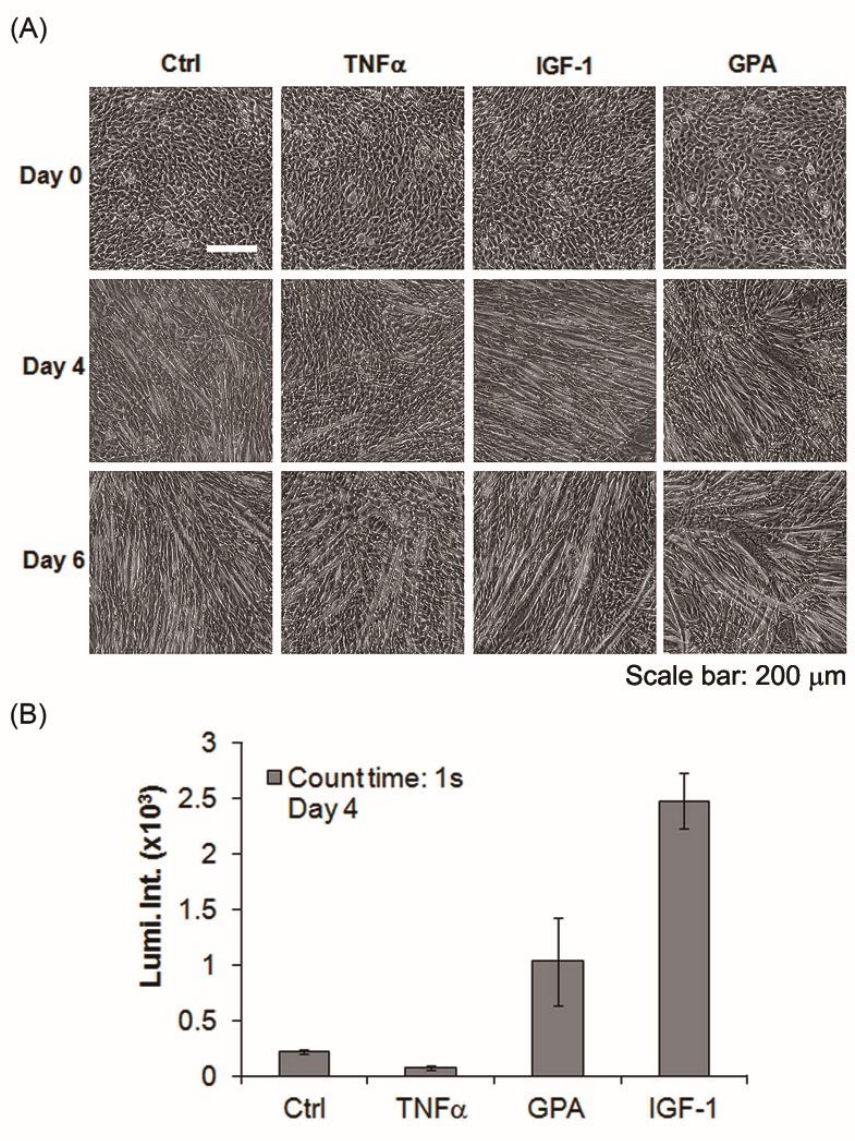


**Fig. 2-10. Chemical compound-induced myogenesis inhibition and promotion of C2C12 cells.** (A) Myotubes formed in the mixture of N-cells and C-cells treated with TNFα, IGF-1 or GPA; (B) Luminescence intensities (± SD, n = 10) from the mixture of N-cells and C-cells which were treated with TNFα, IGF-1, and GPA. 0.2 mmol $L^{-1}$ D-luciferin was used for luminescence measurement.

### 2-3-7. Effects of dimethyl sulfoxide on myogenesis of C2C12 cell

In chemical libraries, compounds are usually pre-dissolved in dimethyl sulfoxide (DMSO) at a high concentration and diluted highly for screening. Since it is unclear that how much DMSO will affect myogenesis of N-cells and C-cells, the concentration-dependent effect on the myogenesis of N-cells and C-cells by DMSO were assessed. The mixture of N-cells and C-cells were induced to differentiate with the differentiation medium added in DMSO at final concentrations of 0, 0.1%, 0.5% and 1.0% (V/V), respectively. The effects of DMSO were assessed through observing the myotube formation with the phase-contrast microscope **(Fig. 2-11A)** and detecting luminescence intensities **(Fig. 2-11B)** from each of the test samples. Both assessments suggest that 0.1% DMSO does not affect the myogenesis of C2C12 cells, whereas DMSO more than 0.5% in concentration will obviously inhibit the myogenesis.

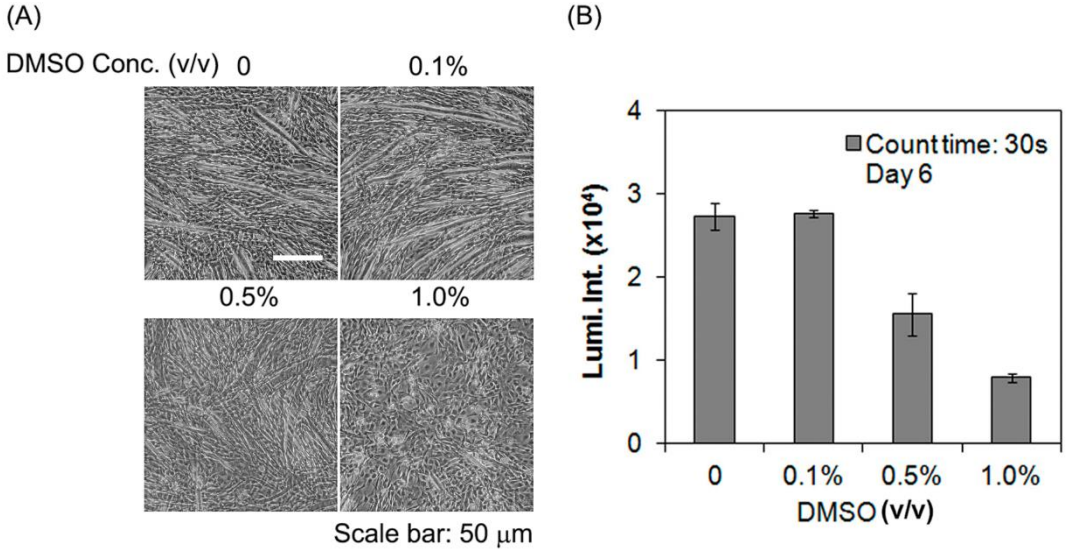


**Fig. 2-11. Effects of DMSO on myotube formation and luminescence intensity of the mixture of N-cells and C-cells.** Phase-contrast images (A) and luminescence intensities (±SD, *n*=2) (B) were obtained for the N-C cell mixture cultivated with varying concentration of DMSO and differentiated for 6 Days.

### 2-3-8. Evaluation of the 96-well plate-based assay for high-throughput screening of myogenesis-promoting chemical compounds

To validate the robustness and quality of the system in the 96-well plate-based assay, Z'-factor[18,62] was determined. In the determination, DMSO (0.1%) and IGF-1(10 ng $mL^{-1}$) were used as negative and positive controls, respectively. 12 negative controls and 48 positive controls were arranged on one 96-well plate as shown in **Fig. 2-12A** and luminescence intensities counted from corresponding wells were showed on **Fig. 2-12B**. In total, three plates were used to repeat the experiment. Distribution of luminescence intensities of the negative and positive controls were shown in **Fig. 2-12C**. The mean (*Avg*) and standard deviation (*SD*) of the luminescence intensities (*I*) of the positive (+) and negative (-) controls and the coefficient of variation (CV), signal to background ratio (S/B) and Z'-factor further calculated were summarized to **Table 2-1** by plates. As a result, the Z'-factor of 0.44±0.05 (Mean±SD) was determined for the 96-well plate-base assay. Because the value was in the range of acceptance criterion (Z'- factor $\geq$ 0.4),[63] the present system showed a sufficient reliability for 96-well plate-based assay to identify chemical compounds that promote myogenesis with the same efficacy as IGF-1.

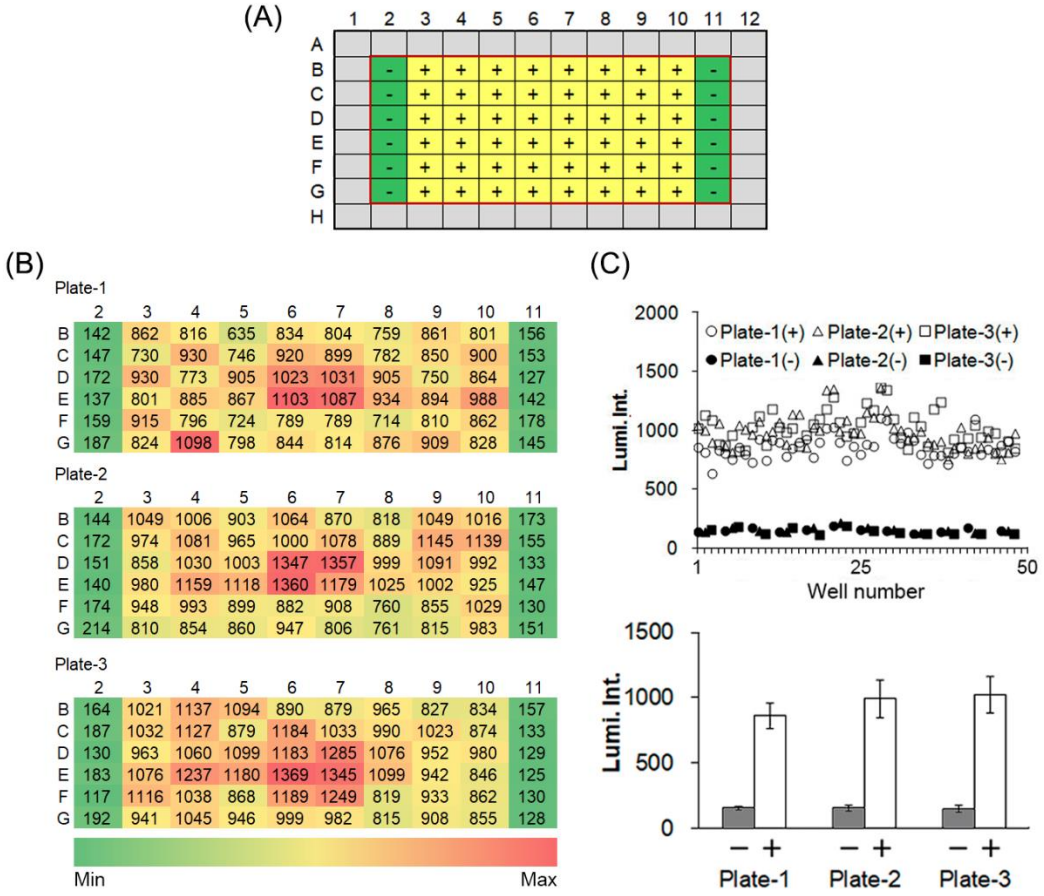


**Fig. 2-12. Validation of a 96-well plate-based assay using for myogenesis-promoting compounds.** (A) The layout of the 96-well plate for the assay. (+) and (-) represent positive and negative control, respectively. Luminescence intensity was counted for the wells within the red box; (B) Heatmaps of the luminescence intensity measured on each test plates; (C) Scatter plot and column chart of the luminescence intensities.

**Table 2-1. The evaluation parameters of the 96-well plate-based high-throughput screening.**

| Plate No. | | $I_{Avg}$ | $I_{SD}$ | CV (%) | S/B | Z'-factor |
|---|---|---|---|---|---|---|
| 1 | - | 154 | 18 | **11** | **5.6** | **0.50** |
| | + | 859 | 100 | **12** | | |
| 2 | - | 157 | 23 | **15** | **6.3** | **0.41** |
| | + | 991 | 141 | **14** | | |
| 3 | - | 148 | 27 | **18** | **6.9** | **0.42** |
| | + | 1022 | 143 | **14** | | |

"-": negative ctrl;

"+": positive ctrl;

$I_{Avg}$: mean of luminescence intensity;

$I_{SD}$: standard deviation of luminescence intensity

CV: coefficient of variation

S/B: signal to background ratio

$$\mathrm{CV}(\%) = \frac{I_{SD}}{I_{Avg}} \times 100\%$$

$$\mathrm{S/B} = \frac{I_{Avg}^{C+}}{I_{Avg}^{C-}}$$

$$\mathrm{Z'\text{-}factor} = 1 - \frac{3(I_{SD}^{C+} - I_{SD}^{C-})}{\left|I_{Avg}^{C+} - I_{Avg}^{C-}\right|}$$

## 2-4. Conclusions

A luminescence-based myogenesis assay system which used protein trans-splicing and split Fluc reconstitution techniques was demonstrated. The system comprises two stable C2C12 cell lines (N-cell and C-cell) which are respectively harboring the probe proteins involving FlucN (N-probe) and that involving FlucC (C-probe). In the system, the N-cells and C-cells were mixed in equal amount to induce myogenesis and the luminescence signal was emitted only when the N-cells fused with C-cells. This is because the fusion between N-cell and C-cell enabled the spontaneous reconstitution of Fluc by the N-probe and C-probe. And the reconstitution relied on the split DnaE intein part of the probes, which connected FlucN and FlucC covalently via a *trans*-splicing reaction. Because the luminescence intensity was linearly correlated to the cell fusion frequency represented by the fusion index, which is widely and conventionally used the indicator for myogenesis, the myogenesis extent can be quantitatively assessed via the luminescence intensity. Besides, the system can also reflect the myogenesis-promotion or inhibition effects of chemical compounds such as IGF-1, GPA, and TNFα, indicating that it is capable for screening myogenesis-promoting compounds. For application to the screening in a high-throughput manner, the present system showed a competent robustness and quality in the 96-well plate scale assay since the Z'-factor was determined as 0.44±0.05 (Mean±SD), which was in the range of acceptance criterion (Z'- factor ≥ 0.4).

# Chapter 3

# Application of the 96-well plate-based assay to the screening of myogenesis-promoting compounds in a chemical library

## 3-1. Introduction

In the previous assessment, the 96-well plate-based myogenesis assay consisted of N-cell and C-cell were confirmed if applicable for the screening of myogenesis-promoting compounds in a high-throughput manner. The purpose of developing such a myogenesis assay was to expediently discover of drug candidates for the muscle wasting diseases. Therefore, the application of this assay in screening chemical compounds that promote myogenesis in a chemical library was proved here. In this screening investigation, 1,191 pharmacologically-proven bioactive molecules (Prestwick Chemical)[64] were tested in total. And, the library compounds were used for screening at a concentration of 5 μmol $L^{-1}$, resulting in two hit compounds, Imatinib and Doxazosin mesylate. The two compounds were further assessed for their dose-dependent extent for on the myogenesis on N-cell, C-cell and the intact C2C12 cell. Although Imatinib and Doxazosin mesylate were newly found of their effects on promoting the myogenesis of C2C12 cells, a few theoretical clues were found to support the myogenesis-promoting effect from the previous studies. Therefore, it was demonstrated that the present system is not only theoretically applicable but also indeed useful in finding myogenesis-promoting chemical compounds.

## 3-2. Materials and Methods

### 3-2-1. Materials

The chemical library was provided by Prestwick Chemical PC SAS (Illkirch-Graffenstaden, France). Imatinib and Doxazosin mesylate were purchased from Tokyo Chemical Industry Co., Ltd. (Tokyo, Japan). Other materials were all mentioned in **Section 2-2-1**.

### 3-2-2. Procedure of screening

In advance, 0.5 μL aliquots were prepared for each of the library chemicals (5 mmol $L^{-1}$ in DMSO). When used, the aliquots were diluted with 200 μL differentiation medium to make a compound-containing medium. The N-cells and C-cells was mixed at 1:1 (n/n) homogeneously and seeded to a white opaque 96-well plate at $1.4 \times 10^4$ cells per well. The cells were cultured for two days to reach full confluence and washed with 200 μL PBS once. And then, to induce the differentiation of the cells and test the chemical samples, 120 μL of the differentiation medium and 80 μL of the above-mentioned compound-containing medium were added to each well, successively. Thus, the final concentration of the chemical compound is 5 μmol $L^{-1}$(1:1000 diluted from the initial concentration). After 2 days of cell culture, the medium was changed in the same way but without the washing step. 4 days after differentiation induction, the differentiation medium was removed, and the wells were washed once with 200 μL of PBS. At last, 100 μL of a substrate solution (0.2 mmol $L^{-1}$ D-luciferin in a phenol red-free DMEM) was added to each well and the luminescence intensity was detected well-by-well immediately for 1 s per well by the microplate multimode reader. The measurement was repeated for five times until the luminescence intensities reached

plateaus, which took 10 min for one plate. The average of the five measurements was calculated as the luminescence intensity corresponding to the chemical sample. DMSO was used as negative control sample while IGF-1 as positive control sample. The concentration of DMSO in all wells were kept consistent at 0.1%.

### 3-2-3. Preparation of varying concentrations of compound-containing mediums

10 mmol $L^{-1}$ stock solutions of Imatinib and Doxazosin mesylate were prepared by pre-dissolving the compounds in DMSO. When used, the stock solutions were diluted with the differentiation medium into a 10 μmol $L^{-1}$ working solution. And from the working solution and the differentiation medium added DMSO at final concentration of 0.1%, varying concentrations of the compound-containing mediums were prepared. Thus, the concentration of DMSO in all the compound-containing medium was kept consistent at 0.1%.

### 3-2-4. Assessment of dose-dependent effects by Imatinib and Doxazosin by the 96-well plate-based assay

The N-cells and C-cells was mixed at 1:1 (n/n) homogeneously and seeded to a white opaque 96-well plate at $1.4 \times 10^4$ cells per well. The cells were cultured for two days to reach full confluence and washed with 200 μL of PBS once. And then, varying concentrations of the compound-containing mediums were used as the differentiation medium. 4 days after inducting the differentiation, the luminescence intensity was measured (see **Section 3-2-2**).

### 3-2-4. Assessment of dose-dependent effects by Imatinib and Doxazosin mesylate on myogenesis of intact C2C12 cells through fusion index

The cells were seeded to a 48-well plate at $4.0 \times 10^4$ cells per well to conduct the differentiation. And different concentrations of the compound-containing mediums were used as the differentiation medium. Six days after differentiation induction, the phase-contrast images of the cell cultures under CKX31N-11PHP phase-contrast microscope (Olympus Corp., Tokyo, Japan) which was mounted UPlanFLN 4x objective lens (Olympus Corp.), were obtained by the XZ-2 CKX31N-11PHPdigital camera (Olympus Corp.), mounted an NY-XZ1 microscope adapter (Olympus Corp.). And then, the nuclei and myotubes in the cell culture were indicated via the immunofluorescence (see **Section 2-2-9** for the details) by using the FLUOVIEW FV1200 biological laser scanning microscope (Olympus Corp., Tokyo, Japan), which was mounted LUCPLANFLN 20x objective lens (Olympus Corp.) (for normal polystyrene plates). Based on the imaging data, numbers of nuclei inside and outside myotubes were detected, and the fusion index was calculated.

## 3-3. Results and discussion

### 3-3-1. Screening library chemical compounds for myogenesis-promoting compounds

1,191 pharmacologically-proven bioactive molecules (S) were tested by using the 96-well plates-based assay based on the present myogenesis evaluating system. The chemical compounds were provided in DMSO, which were all 5 mmol $L^{-1}$. They were added into the differentiation medium where the final concentration was 5 μmol $L^{-1}$ (1:1000 diluted). Thus, DMSO (0.1%) was used as the negative control sample (C-). This time, IGF-1 (10 ng $mL^{-1}$) were used as the positive control sample (C+) where DMSO contained was also 0.1%, to screen the compounds with comparable myogenesis-promoting efficacy with IGF-1. The luminescence intensity (*I*) detected were normalized to the percent activity via the following equation:

$$\text{Percent activity (\%)} = \frac{I^{S} - I^{C-}}{I^{C+} - I^{C-}} \times 100\%$$

Percent activities which were obtained for the library compounds from the primary screening (n=1) were shown in **Fig. 3-1**, which were summarized into a frequency distribution chart in **Fig. 3-2A**. From the frequency distribution, it was seen that three chemical compounds yielded a percent activity that was higher than 100% (IGF-1). The three compounds were tested again (n=3), and two of them, namely, Imatinib and Doxazosin mesylate, reproduced the previous a high percent activity in **Fig. 3-2B**. According to the percent activity, Imatinib and Doxazosin mesylate should possess comparable myogenesis-promoting efficacy with IGF-1. The myogenesis-promoting

efficacy of the two compounds were further confirmed through phase-contrast observation of the myotube formation in the cell cultures which were respectively treated with Imatinib (5.0 μmol $L^{-1}$) or Doxazosin mesylate (5.0 μmol $L^{-1}$). As a result, wider myotubes were seen in the cell culture treated with either compound comparing to the control sample. **(Fig. 3-2C)** Unlike Imatinib, Doxazosin was tested in the form of mesylate, so there was doubt that whether mesylate influences myogenesis. We summarized the screening results of all mesylate compounds in **Table 3-1**, which is showing that not all the mesylate compounds exhibited the effects of promoting muscle formation. Therefore, it is certain that Doxazosin mesylate promoting myogenesis is resulted by Doxazosin rather than mesylate.

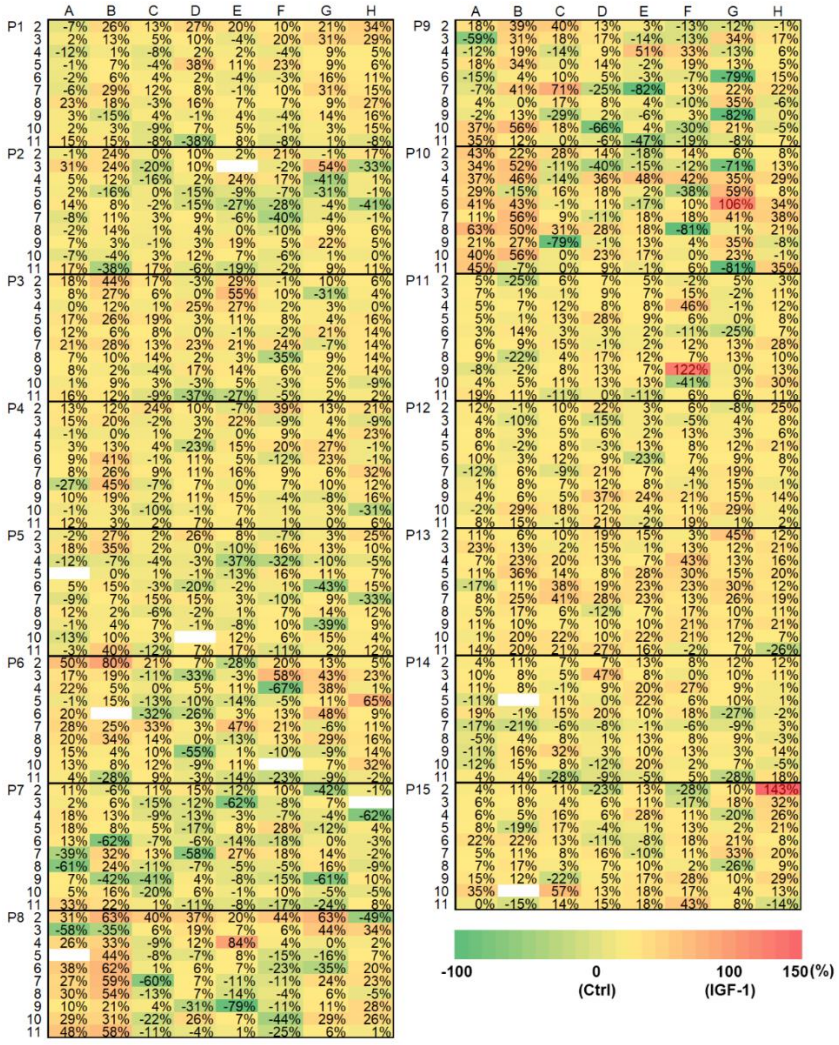


**Fig. 3-1. Heat map of the percent activities obtained for 1,191 chemical compounds.** The percent activity of a compound is shown at the storage location on the plates in Prestwick Chemical Library, thus the plate and well numbers indicates the corresponding compound for each data.

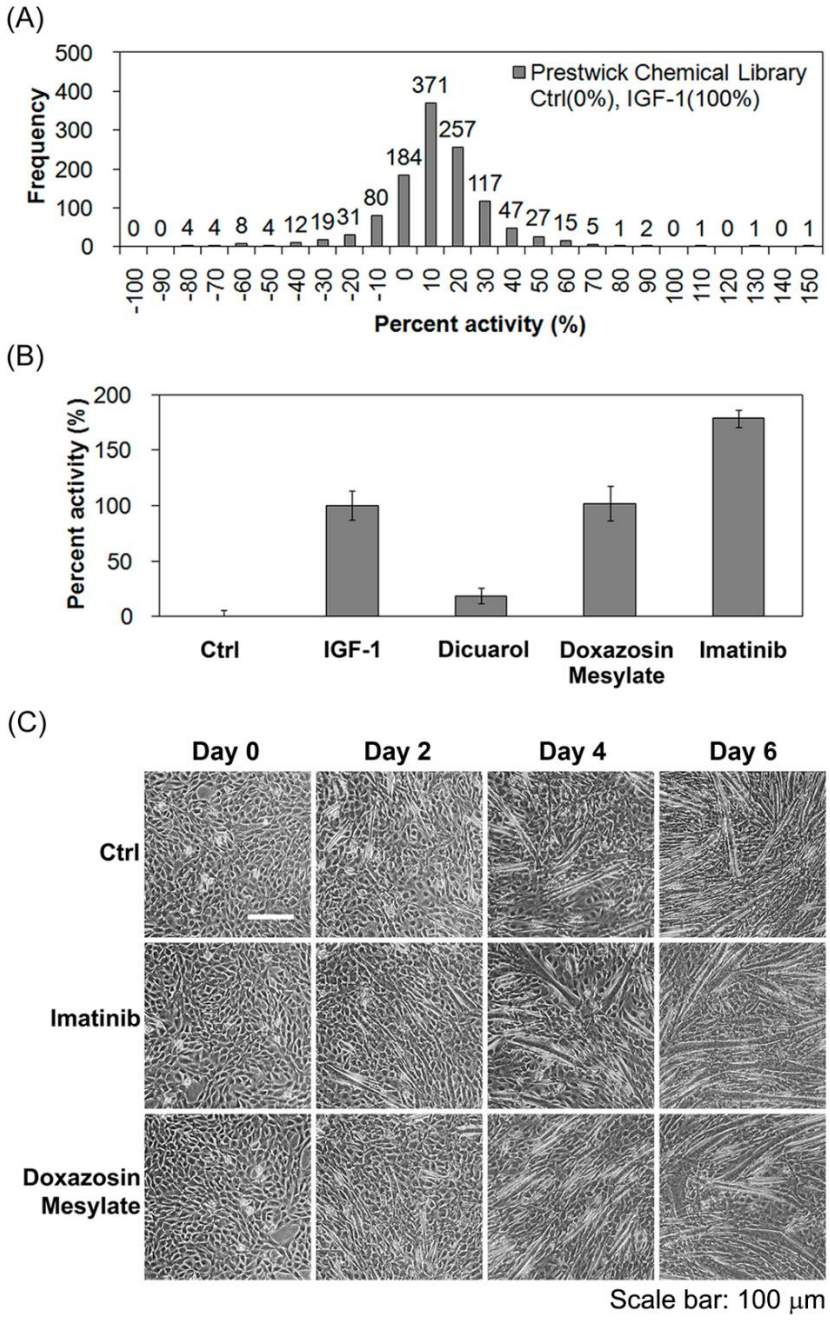


**Fig. 3-2. Screening and discovery of myogenesis-promoting compounds from the chemical library.** (A) Distribution of the percent activities measured for 1,191 chemical compounds. (B) Percent activities (± SD, n = 3) confirmed for three "hit" compounds; (C) Myotubes formed in the mixture of N-cells and C-cells on varying differentiation days under the treatments of Imatinib and Doxazosin mesylate.

**Table 3-1. Mesylate compounds in the Prestwick Chemical Library**

| Prestwick No. | Plate No. / Position No. | Chemical name | Percent activity (%) |
|---|---|---|---|
| Prestw-121 | 02E02 | Bromocryptine mesylate | 2 |
| Prestw-149 | 02G10 | Thioproperazine dimesylate | 1 |
| Prestw-295 | 04F06 | Pergolide mesylate | -12 |
| Prestw-543 | 07G04 | Betahistine mesylate | -4 |
| Prestw-1328 | 08C02 | Reboxetine mesylate | 63 |
| Prestw-725 | 10A06 | Deferoxamine mesylate | 41 |
| Prestw-749 | 10C10 | Isoetharine mesylate salt | 0 |
| Prestw-858 | 11F09 | Doxazosin mesylate | 122 |
| Prestw-973 | 13B04 | Pirlindole mesylate | 23 |
| Prestw-1114 | 14H05 | Saquinavir mesylate | 1 |
| Prestw-1236 | 15F07 | Benztropine mesylate | 11 |

### 3-3-2. Dose-dependent effects of Imatinib and Doxazosin mesylate on the myogenesis assessed with the present system

The dose-dependent effects on the myogenesis by the two hit compounds were investigated by the present 96-well plate-based assay system via luminescence intensity. **(Fig. 3-3)** The mixture of N-cells and C-cells were treated with 0, 1.0, 3.0, 4.0, 5.0, 6.0, 7.0, 8.0 and 9.0 μmol $L^{-1}$ of the compound, respectively. After 4 days of the differentiation, the luminescence intensity was measured. As a result, the optimal concentrations were 6.0 μmol $L^{-1}$ for Imatinib and 4.0 μmol $L^{-1}$ for Doxazosin mesylate, respectively, according to the strength of the luminescence signal produced.

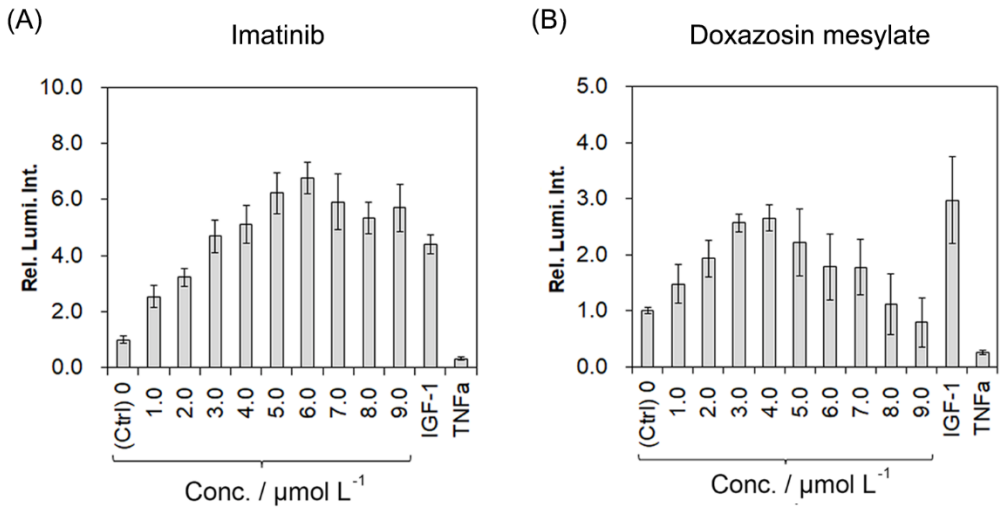


**Fig. 3-3. Dose-dependent variation of luminescence intensity yield from the 96-well plated-base assay system in the cases of Imatinib and Doxazosin mesylate.** Luminescence intensities were shown in the relative values to the negative control sample (±SD, n=5),1.0 mmol $L^{-1}$ D-luciferin was used for the measurement of the luminescence intensity on Day 4.

### 3-3-3. Dose-dependent effects of Imatinib and Doxazosin mesylate on the myogenesis of C2C12 cells

To verify whether the optimum in the concentration of the two compounds obtained by the present luminescence-based system is reliable, and the optimum in promoting the myogenesis of intact C2C12 cells, the myotube formation in the C2C12 samples respectively treated with 0, 0.5, 1.0, 2.0, 4.0, 6.0, 8.0 and 10.0 μmol $L^{-1}$ each compound was assessed via the phase-contrast imaging **(Fig. 3-4A and Fig. 3-5A)**, the immunofluorescence imaging **(Fig. 3-4B and Fig. 3-5B)** and the fusion index **(Fig. 3-4C and Fig. 3-5C)**. Based on observations of the Imatinib-treated samples **(Fig. 3-4)** and Doxazosin mesylate-treated **(Fig. 3-5)** from these three aspects, the optimal concentrations were consistently ascertained, which was 6.0 μmol $L^{-1}$ for Imatinib and 4.0 μmol $L^{-1}$ for Doxazosin mesylate, respectively. In addition, in the light of the phase-contrast images and the decrease of total nuclei, it can be known that the decreased luminescence intensity over the concentration exceeding the optimum value should be attributable to the results of compound-induced cytotoxicity.

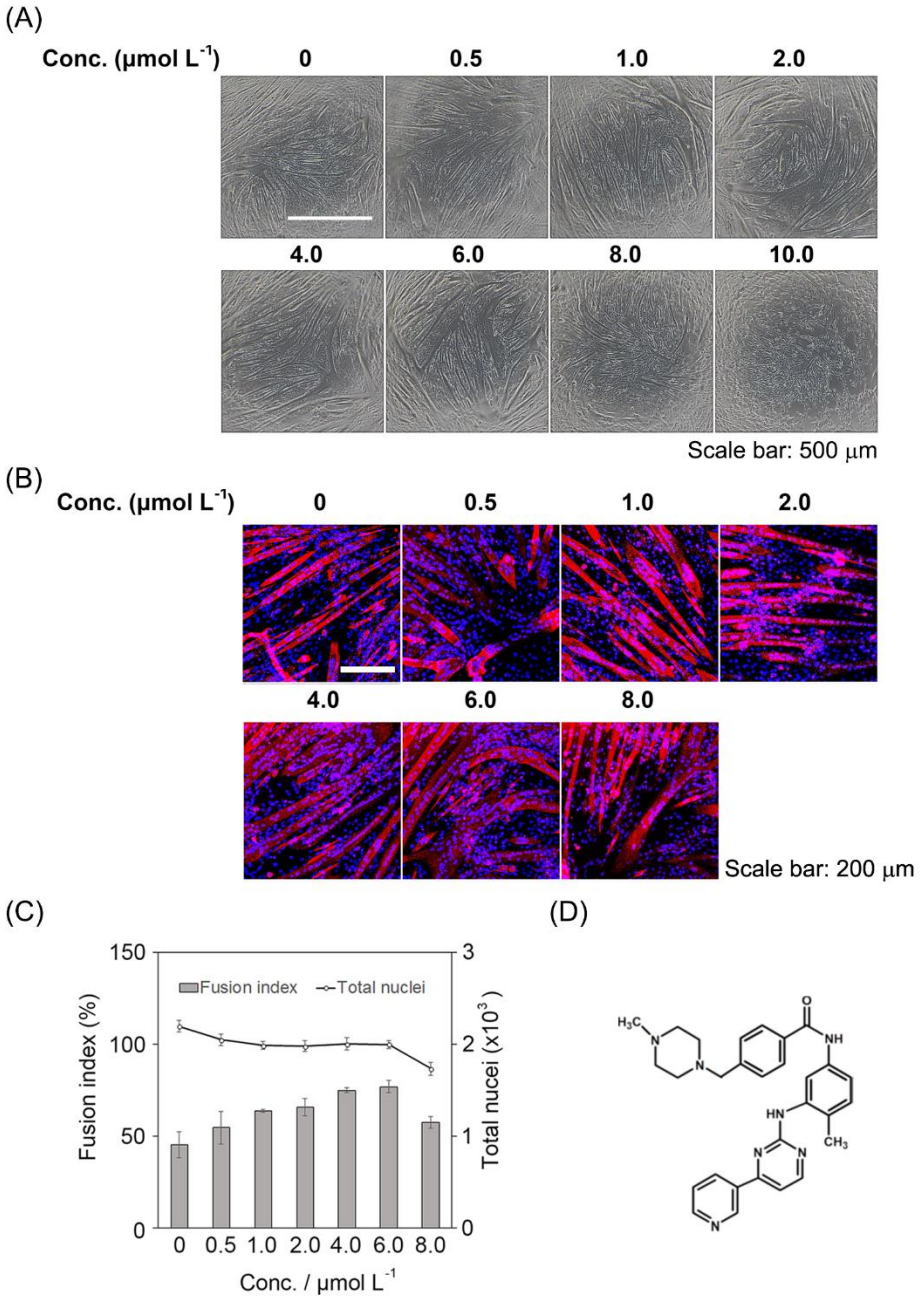


**Fig. 3-4. Dose-dependent effects on myogenesis of C2C12 cells by Imatinib.** (A) Phase-contrast images of the C2C12 cells treated with different concentrations of Imatinib. (B) Immunofluorescence images of the above mentioned C2C12 cells. (C) Fusion index and total number of nuclei calculated based on the Immunofluorescence images.

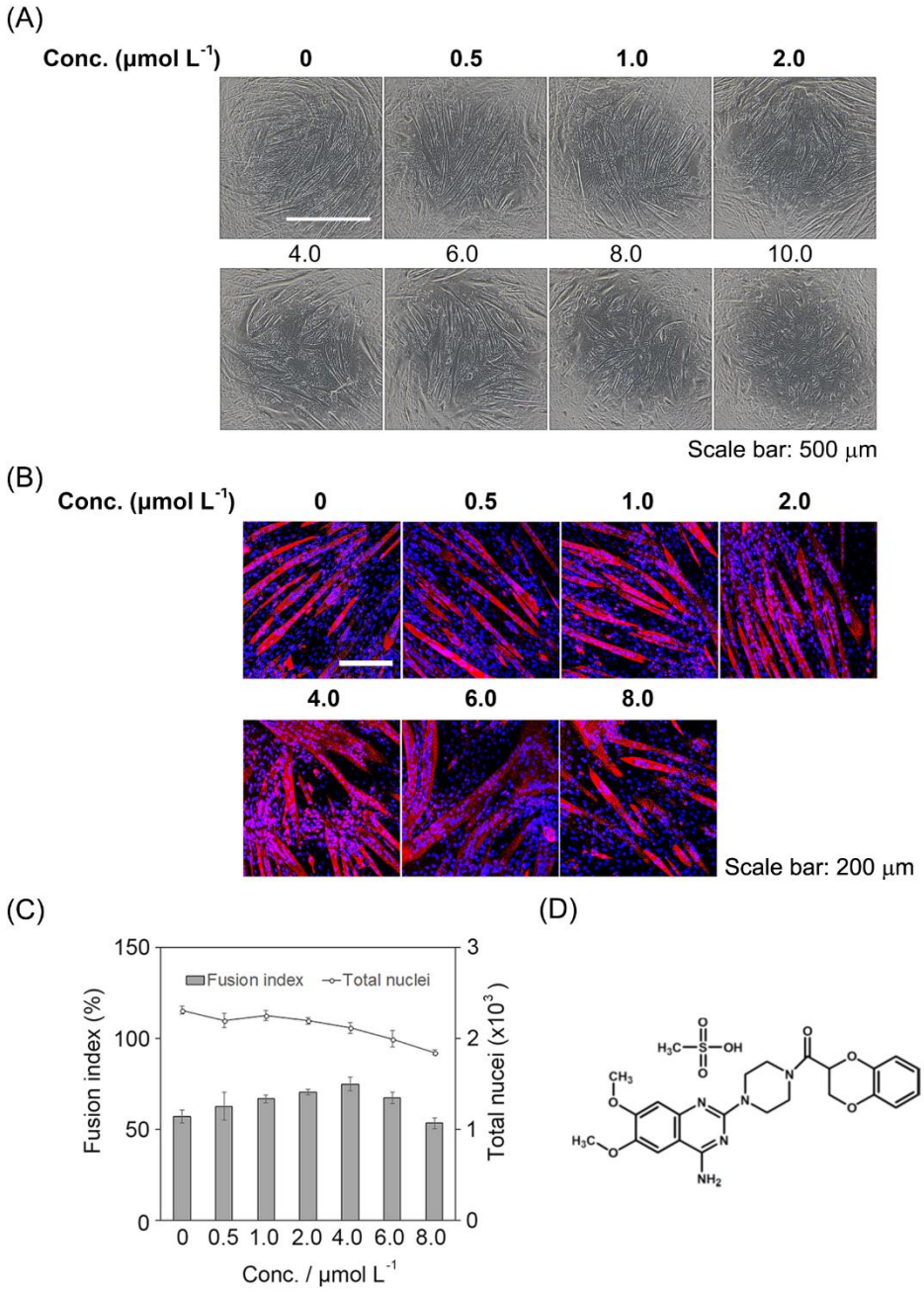


**Fig. 3-5. Dose-dependent effects on myogenesis of C2C12 cells by Doxazosin mesylate.** (A) Phase-contrast images of the C2C12 cells treated with different concentrations of Doxazosin mesylate. (B) Immunofluorescence images of the above mentioned C2C12 cells. (C) Fusion index and total number of nuclei calculated based on the Immunofluorescence images.

### 3-3-4. Discussion

In the screening, to avoid disturbance from the edge effects, the outermost wells in the 96-well plates were not used. Thus, for the test of 1,191 pharmacologically-proven bioactive molecules (fifteen 96-well plates provided by Prestwick Chemical), thirty 96-well plates were used. And 10 min was cost at luminescence counting for each plate in order to let the luminescence intensity reached a plateau. Thus, 300 min were taken as a result for the whole luminescence measurement. That means, the test speed of the screening system is nearly 5 samples per minute. Comparing to a conventional method based on the microscopy, which takes at least the minutes to take a picture for a sample without considering the other processes such as immunofluorescence and nuclei counting, the present luminescence-based assay method greatly accelerated the assessment of myogenesis progress.

The two chemical compounds screened out by the present assay from the chemical library were also confirmed by robust conventional method for their myogenesis-promoting effects. And as described below, there are several theoretical basis for the role of these two compounds in promoting the myogenesis.

Imatinib, a rationally designed oral signal transduction inhibitor, is a 2-phenyl amino pyrimidine derivative **(Fig. 3-4D)** which is quite selective for Bcr-Abl tyrosine kinases, though it does also inhibit other targets (c-kit and PDGF-R), as well as ABL2 (ARG) and DDR1 tyrosine kinases and NQO2 - an oxidoreductase.[65,66] It occupies the TK active site, leading to a decrease in activity of kinases. Recent studies in patients related to gastrointestinal stromal tumor treated with imatinib showed that sarcopenia (the degenerative loss of skeletal muscle mass, quality, and strength) was reversible.[67] This phenomenon is consistent with the conclusion obtained by the present study that

Imatinib promotes muscle formation. Its mechanism is not clear, but a few clues can be found from previous studies. An earlier study suggested that the p38 mitogen-activated protein kinase (MAPK) pathway is activated by treating BCR/ABL expressing cells with Imatinib.[68] The p38 MAPK pathway plays a critical role in skeletal muscle differentiation.[69,70] Therefore, the myogenesis process promoted by Imatinib might be associated with activation of the p38 MAPK pathway.

Doxazosin mesylate is a quinazoline-derivative **(Fig. 3-5D)** that selectively antagonizes postsynaptic α1-adrenergic receptors.[71] For prostatic smooth muscle cells, doxazosin reportedly has a long-term effect on the differentiation.[72] However, no reports to date have described the effect of Doxazosin mesylate on the differentiation of skeletal muscle cells.

Taking these previous reports together, it can be concluded that both Imatinib and Doxazosin mesylate are all new compounds which promote the myogenesis of skeletal muscle on a cultured-cell level. But, as above mentioned, Imatinib and Doxazosin specifically target at different targets in completely different interaction mechanisms, thus it is incapable to extract the structural similarity which can lead to the promotion of muscle formation from the chemical structure of the two.

## 3-4. Conclusion

By applying the 96-well plate based myogenesis-assay system to the screening of myogenesis-promoting compounds from 1,191 pharmacologically-proven bioactive molecules (Prestwick Chemical) under the concentration of 5 μmol $L^{-1}$, two compounds, Imatinib and Doxazosin mesylate, were found to possess the myogenesis-promoting property comparable to IGF-1. The two compounds were further evaluated for their dose-dependent effects on the myogenesis of N-cell, C-cell and the intact C2C12 cell, and the optimum concentrations were consistently ascertained to be 6.0 μmol $L^{-1}$ for Imatinib and 4.0 μmol $L^{-1}$ for Doxazosin mesylate, respectively. Both Imatinib and Doxazosin mesylate were newly found myogenesis-promoting compound for C2C12 cells, and a few theoretical clues were found to support the myogenesis-promoting fact from the previous studies. Consequently, the researched result manifested that the present system is not only theoretically applicable but also indeed useful in finding myogenesis-promoting chemical compounds.

# Chapter 4

# General conclusion

In this study, a luminescence-based myogenesis assay system which used protein *trans*-splicing-based split Fluc reconstitution techniques was demonstrated. In the system, the N-probe and C-probe consisted of complementary Fluc fragment and split intein were generated, and the N-cell and C-cell were prepared by harboring either of the probes to the C2C12 cell, which is widely used as myogenesis model cell. When the mixture of N-cells and C-cells was induced myogenesis (the differentiation process accompanied with cell fusions), the N-cell and C-cell fused together to make the two types of probes accessible to each other. This resulted in the trigger of protein *trans*-splicing by split intein parts of the probes, covalently connecting two complementary Fluc fragments to reconstitute Fluc that can emit the luminescence signal. The luminescence intensity was linearly correlated to the cell fusion frequency represented by the fusion index which is a widely and conventionally used indicator for the myogenesis. The linear correlation between the luminescence intensity and the cell fusion frequency was dependable under the addition of myogenesis-promotion/inhibition chemical compounds such as IGF-1, GPA, and TNFα, indicating that the present system can be used for screening myogenesis-inducible compounds. Using the myogenesis assay system consisted of N-cell and C-cell, the screening of 1,191 of pharmacologically proven bioactive chemical compounds was demonstrated, and Imatinib and Doxazosin mesylate, were identified as myogenesis-inducible drugs which were higher in efficacies than IGF-1 as a result.

Prominent features of the present myogenesis-assay system are robustness and rapidity. A conventional and robust approach to evaluate the myogenesis is based on the direct microscopy observation of cell fusion. The fusion index, which is estimated upon microscopic observation and represents the number of the fused cells in

myogenesis process, is widely used as a direct and robust indicator for myogenesis. The luminescence intensities in the present myogenesis assay displayed strong linear correlation to the fusion index. Furthermore, in the case of the 96-well plate assay, luminescence signals were acquired within 1 s from individual well. Such rapidity in data-acquisition allows the present system can be used to the high-throughput screening of chemical compounds. In addition, the method developed by using Fluc and *Synechocystis* sp. PCC6803 split DnaE intein was demonstrated to be applicable for the identification of compounds possessing the myogenesis-promoting effect comparable to IGF-1. Theoretically speaking, the sensitivity of the method should be improved by substituting Fluc with a luminescence protein which has higher luminous efficiency and replacing the *Synechocystis* sp. PCC6803 split DnaE intein with other split inteins which have more efficient protein splicing efficiency. Thus, by the above improvements, it is expected that the method can also be used for screening of compounds having a lower promoting effect compare with IGF-1, such as GPA. Fluorescence-based assay is also applied for screening in the chemical libraries. However, considering fluorescence properties of many chemical compounds, the luminescence assay is ideal for chemical compound screening. Thus, the present myogenesis assay system provides a promising approach for identification of myogenesis-promoting agents through a robust high-throughput screening.

In summary, I verified the feasibility of the present method in the evaluation of muscle formation. However, as a system for monitoring the cell fusion, the application of the system is not limited to studies related to muscle formation, such as skeletal muscle tissue engineering and drug screening as described above, but may also be used for evaluating other processes involving cell fusion, such as the formation of bones

and placenta, the regeneration of liver, bones and cartilage,[73] the development of model organisms (such as *Caenorhabditis elegans*)[74] and the fusion of cancer cell-stromal cells[75]. Especially in the case of synkaryons formation, the cell fusion accompanied with fusion of nuclei, which recently received great attention because it could explain the genesis of some tumors, the evaluation through the fusion index cannot work. Therefore, the present method system would have broader application prospects comparing with the traditional methods.

# References


(1) Janssen, I., Heymsfield, S. B., Wang, Z. M., and Ross, R. (2000) Skeletal muscle mass and distribution in 468 men and women aged 18-88 yr. *J. Appl. Physiol. 89*, 81–88.

(2) Ostrovidov, S., Hosseini, V., Ahadian, S., Fujie, T., Parthiban, S. P., Ramalingam, M., Bae, H., Kaji, H., and Khademhosseini, A. (2014) Skeletal muscle tissue engineering: methods to form skeletal myotubes and their applications. *Tissue Eng. 20*, 403–436.

(3) Le Grand, F., and Rudnicki, M. A. (2007) Skeletal muscle satellite cells and adult myogenesis. *Curr. Opin. Struct. Biol. 19*, 628–633.

(4) Evans, W. J. (2010) Skeletal muscle loss: cachexia, sarcopenia, and inactivity. *Am. J. Clin. Nutr. 91*, 1123S–1127S.

(5) Dumont, N. A., Wang, Y. X., and Rudnicki, M. A. (2015) Intrinsic and extrinsic mechanisms regulating satellite cell function. *Development 142*, 1572–1581.

(6) Andrs, V., and Walsh, K. (1996) Myogenin expression , cell cycle withdrawal, and phenotypic differentiation are temporally separable events that precede cell fusion upon myogenesis. *J. Cell Biol. 132*, 657–666.

(7) Nguyen, N.-U.-N., and Wang, H.-V. (2015) Dual roles of palladin protein in in vitro myogenesis: inhibition of early induction but promotion of myotube maturation. *PLoS One 10*, e0124762.

(8) Pomi Es, P., Rodriguez, J., Blaqui Ere, M., Sedraoui, S., Gouzi, F., Carnac, G., Laoudj-Chenivesse, D., Mercier, J., Pr Efaut, C., and Hayot, M. (2015) Reduced myotube diameter, atrophic signalling and elevated oxidative stress in cultured

satellite cells from COPD patients. *J. Cell Mol. Med. 19*, 175–186.

(9) Agley, C. C., Velloso, C. P., Lazarus, N. R., and Harridge, S. D. R. (2012) An image analysis method for the precise selection and quantitation of fluorescently labeled cellular constituents: application to the measurement of human muscle cells in culture. *J. Histochem. Cytochem. 60*, 428–438.

(10) Bajaj, P., Reddy, B., Millet, L., Wei, C., Zorlutuna, P., Bao, G., and Bashir, R. (2011) Patterning the differentiation of C2C12 skeletal myoblasts. *Integr. Biol. 3*, 897–909.

(11) Pajcini, K. V, Pomerantz, J. H., Alkan, O., Doyonnas, R., and Blau, H. M. (2008) Myoblasts and macrophages share molecular components that contribute to cell–cell fusion *180*, 1005–1019.

(12) Veliça, P., and Bunce, C. M. (2011) A quick, simple and unbiased method to quantify C2C12 myogenic differentiation. *Muscle and Nerve 44*, 366–370.

(13) Miyake, T., McDermott, J. C., and Gramolini, A. O. (2011) A method for the direct identification of differentiating muscle cells by a fluorescent mitochondrial dye. *PLoS One 6*, e28628.

(14) Kodaka, M., Yang, Z., Nakagawa, K., Maruyama, J., and Xu, X. (2015) A new cell-based assay to evaluate myogenesis in mouse myoblast C2C12 cells. *Exp. Cell Res. 336*, 171–181.

(15) Kodaka, M., Xu, X., Yang, Z., Maruyama, J., and Hata, Y. (2017) Application of Split-GFP Reassembly Assay to Study Myogenesis and Myofusion In Vitro. *Methods Mol Bio. 1668*, 127–134.

(16) Thorne, N., Inglese, J., and Auld, D. S. (2010) Illuminating insights into firefly luciferase and other bioluminescent reporters used in chemical biology. *Chem. Biol.*

*17*, 646–657.

(17) Yu, W., and Hardin, P. E. (2007) Use of firefly luciferase activity assays to monitor circadian molecular rhythms in vivo and in vitro. *Methods Mol Bio. 362*, 465–480.

(18) Li, J.-F., Bush, J., Xiong, Y., Li, L., and McCormack, M. (2011) Large-scale protein-protein interaction analysis in arabidopsis mesophyll protoplasts by split firefly luciferase complementation. *PLoS One* (Somers, D. E., Ed.) *6*, e27364.

(19) Tiffen, J. C., Bailey, C. G., Ng, C., Rasko, J. E., and Holst, J. (2010) Luciferase expression and bioluminescence does not affect tumor cell growth in vitro or in vivo. *Mol. Cancer 9*, 299–306.

(20) Ando, Y., Niwa, K., Yamada, N., Enomoto, T., Irie, T., Kubota, H., Ohmiya, Y., and Akiyama, H. (2008) Firefly bioluminescence quantum yield and colour change by pH-sensitive green emission. *Nat. Photonics 2*, 44–47.

(21) Kim, J., and Somers, D. E. (2010) Rapid assessment of gene function in the circadian clock using artificial microRNA in arabidopsis mesophyll protoplasts. *Plant Physiol. 154*, 611–621.

(22) Pichler, A., Prior, J. L., and Piwnica-Worms, D. (2004) Imaging reversal of multidrug resistance in living mice with bioluminescence: MDR1 P-glycoprotein transports coelenterazine. *Proc. Nati. Acad. Sci. 101*, 1702–1707.

(23) Fan, F., and Wood, K. (2007) Bioluminescent assays for high-throughput screening. *Assay Drug Dev. Technol. 5*, 127–136.

(24) Razgulin, A., Ma, N., and Rao, J. (2011) Strategies for in vivo imaging of enzyme activity: an overview and recent advances. *Chem. Soc. Rev. 40*, 4186–4216.

(25) Fukutani, Y., Ishii, J., Kondo, A., Ozawa, T., Matsunami, H., and Yohda, M.

(2017) Split luciferase complementation assay for the analysis of G protein-coupled receptor ligand response in *Saccharomyces cerevisiae*. *Biotechnol. Bioeng. 114*, 1354–1361.

(26) Takenouchi, O., Kanno, A., Takakura, H., Hattori, M., and Ozawa, T. (2016) Bioluminescent Indicator for Highly Sensitive Analysis of Estrogenic Activity in a Cell-Based Format. *Bioconjug. Chem. 27*, 2689–2694.

(27) Luker, K. E., Smith, M. C. P., Luker, G. D., Gammon, S. T., Piwnica-Worms, H., and Piwnica-Worms, D. (2004) Kinetics of regulated protein–protein interactions revealed with firefly luciferase complementation imaging in cells and living animals. *Proc. Nati. Acad. Sci. 101,* 12288–12293.

(28) Kim, S. B., Awais, M., Sato, M., Umezawa, Y., and Tao, H. (2007) Integrated molecule-format bioluminescent probe for visualizing androgenicity of ligands based on the intramolecular association of androgen receptor with its recognition peptide. *Anal. Chem. 79,* 1874–1880.

(29) Kim, S. B., Kanno, A., Ozawa, T., Tao, H., and Umezawa, Y. (2007) Nongenomic activity of ligands in the association of androgen receptor with Src. *ACS Chem. Biol. 2,* 484–492.

(30) Paulmurugan, R., and Gambhir, S. S. (2005) Firefly luciferase enzyme fragment complementation for imaging in cells and living animals. *Anal. Chem. 77,* 1295–1302.

(31) Ozawa, T., Kaihara, A., Sato, M., Tachihara, K., and Umezawa, Y. (2001) Split luciferase as an optical probe for detecting protein−protein interactions in mammalian cells based on protein splicing. *Anal. Chem. 73*, 2516–2521.

(32) Gehl, C., Kaufholdt, D., Hamisch, D., Bikker, R., Kudla, J., Mendel, R. R., and

Hänsch, R. (2011) Quantitative analysis of dynamic protein-protein interactions in planta by a floated-leaf luciferase complementation imaging (FLuCI) assay using binary Gateway vectors. *Plant J. 67*, 542–553.

(33) Fujikawa, Y., and Kato, N. (2007) Split luciferase complementation assay to study protein-protein interactions in Arabidopsis protoplasts. *Plant J. 52*, 185–195.

(34) Stains, C. I., Furman, J. L., Porter, J. R., Rajagopal, S., Li, Y., Wyatt, R. T., and Ghosh, I. (2010) A general approach for receptor and antibody-targeted detection of native proteins utilizing split-luciferase reassembly. *ACS Chem. Biol. 5*, 943–952.

(35) Paulmurugan, R., Umezawa, Y., and Gambhir, S. S. (2002) Noninvasive imaging of protein-protein interactions in living subjects by using reporter protein complementation and reconstitution strategies. *Proc. Natl. Acad. Sci. U. S. A. 99*, 15608–15613.

(36) Yoshimura, H., and Ozawa, T. (2014) Methods of Split Reporter Reconstitution for the Analysis of Biomolecules. *Chem. Rec. 14*, 492–501.

(37) Kane, P. M., Yamashiro, C. T., Wolczyk, D. F., Neff, N., Goebl, M., and Stevens, T. H. (1990) Protein splicing converts the yeast TFP1 gene product to the 69-kD subunit of the vacuolar H(+)-adenosine triphosphatase. *Science 250*, 651–657.

(38) Hirata, R., Ohsumk, Y., Nakano, A., Kawasaki, H., Suzuki, K., and Anraku, Y. (1990) Molecular structure of a gene, VMA1, encoding the catalytic subunit of H(+)-translocating adenosine triphosphatase from vacuolar membranes of Saccharomyces cerevisiae. *J. Biol. Chem. 265*, 6726–6733.

(39) Mills, K. V, Johnson, M. A., and Perler, F. B. (2014) Protein plicing: show inteins escape from precursor proteins. *J. Biol. Chem. 289*, 14498–14505.

(40) Yaffe, D., and Saxel, O. (1977) Serial passaging and differentiation of myogenic cells isolated from dystrophic mouse muscle. *Nature 270*, 725–727.

(41) McMahon, D. K., Anderson, P. A., Nassar, R., Bunting, J. B., Saba, Z., Oakeley, A. E., and Malouf, N. N. (1994) C2C12 cells: biophysical, biochemical, and immunocytochemical properties. *Am. J. Physiol. 266*, C1795-1802.

(42) Rajan, S., Dang, H. C. P., Djambazian, H., Zuzan, H., Fedyshyn, Y., Ketela, T., Moffat, J., Hudson, T. J., and Sladek, R. (2012) Analysis of early C2C12 myogenesis identifies stably and differentially expressed transcriptional regulators whose knock-down inhibits myoblast differentiation. *Physiol. Genomics 44*, 183–197.

(43) Burattini, S., Ferri, P., Battistelli, M., Curci, R., Luchetti, F., and Falcieri, E. (2004) C2C12 murine myoblasts as a model of skeletal muscle development: morpho-functional characterization. *Eur. J. Histochem. 48*, 223–234.

(44) Cabane, C., Englaro, W., Yeow, K., Ragno, M., and Dérijard, B. (2003) Regulation of C2C12 myogenic terminal differentiation by MKK3/p38α pathway. *Am. J. Physiol. Physiol. 284*, C658-666.

(45) Yaffe, D., and Saxel, O. (1977) A myogenic cell line with altered serum requirements for differentiation. *Differentiation. 7*, 159–166.

(46) Luchetti, F., Gregorini, A., Papa, S., Burattini, S., Canonico, B., Valentini, M., and Falcieri, E. (1998) The K562 chronic myeloid leukemia cell line undergoes apoptosis in response to interferon-alpha. *Haematologica 83*, 974–980.

(47) Luchetti, F., Burattini, S., Ferri, P., Papa, S., and Falcieri, E. (2002) Actin involvement in apoptotic chromatin changes of hemopoietic cells undergoing hyperthermia. *Apoptosis 7*, 143–52.

(48) Zamai, L., Burattini, S., Luchetti, F., Canonico, B., Ferri, P., Melloni, E., Gonelli, A., Guidotti, L., Papa, S., and Falcieri, E. (2004) In vitro apoptotic cell death during erythroid differentiation. *Apoptosis 9*, 235–246.

(49) Burattini, S., Luchetti, F., Battistelli, M., Della Felice, M., Papa, S., Piersanti, G., Tarzia, G., and Falcieri, E. (2003) 5-(2-Ethyl-phenyl)-3-(3-methoxy-phenyl)-1H-[1,2,4]triazole (DL-111-IT) and related compounds induce apoptotic patterns in cultures of human tumor cell lines. *J. Biol. Regul. Homeost. Agents 17*, 348–357.

(50) Kanno, A., Yamanaka, Y., Hirano, H., Umezawa, Y., and Ozawa, T. (2007) Cyclic luciferase for real-time sensing of caspase-3 activities in living mammals. *Angew. Chemie 119*, 7739–7743.

(51) Wu, H., Hu, Z., and Liu, X.-Q. (1998) Protein trans-splicing by a split intein encoded in a split DnaE gene of Synechocystis sp. PCC6803. *Proc. Natl. Acad. Sci. 95*, 9226–9231.

(52) Volkmann, G., and Iwaï, H. (2010) Protein trans-splicing and its use in structural biology: opportunities and limitations. *Mol. Biosyst. 6*, 2110–2121.

(53) Cowan, J. L., and Morley, S. J. (2004) The proteasome inhibitor, MG132, promotes the reprogramming of translation in C2C12 myoblasts and facilitates the association of hsp25 with the eIF4F complex. *Eur. J. Biochem. 271*, 3596–3611.

(54) Sun, L., Trausch-Azar, J. S., Ciechanover, A., and Schwartz, A. L. (2005) Ubiquitin-proteasome-mediated degradation, intracellular localization, and protein synthesis of MyoD and Id1 during muscle differentiation. *J. Biol. Chem. Chem. 280*, 26448–26456.

(55) Sun, Y., Ge, Y., Drnevich, J., Zhao, Y., Band, M., and Chen, J. (2010) Mammalian target of rapamycin regulates miRNA-1 and follistatin in skeletal myogenesis. *J.*

*Cell Biol. 189*, 1157–1169.

(56) Ohira, Y., Matsuoka, Y., Kawano, F., Higo, Y., Ohira, T., Terada, M., Oke, Y., Igo, Y. H., Hira, T. O., Erada, M. T., Ke, Y. O., and Akai, N. N. (2011) Effects of creatine and its analog , β-guanidinopropionic acid , on the differentiation of and nucleoli in myoblasts on the differentiation of and nucleoli in myoblasts. *Biosci. Biotechnol. Biochem. 75*, 1085–1089.

(57) Baumgarner, B. L., Nagle, A. M., Quinn, M. R., Farmer, A. E., and Kinsey, S. T. (2015) Dietary supplementation of β-guanidinopropionic acid (βGPA) reduces whole-body and skeletal muscle growth in young CD-1 mice. *Mol. Cell. Biochem. 403*, 277–285.

(58) Latres, E., Amini, A. R., Amini, A. A., Griffiths, J., Martin, F. J., Wei, Y., Hsin, C. L., Yancopoulos, G. D., and Glass, D. J. (2005) Insulin-like growth factor-1 (IGF-1) inversely regulates atrophy-induced genes via the phosphatidylinositol 3-kinase/Akt/mammalian target of rapamycin (PI3K/Akt/mTOR) pathway. *J. Biol. Chem. 280*, 2737–2744.

(59) Miyazaki, M., McCarthy, J. J., and Esser, K. A. (2010) IGF-1-induced phosphorylation and altered distribution of TSC1/ TSC2 in C2C12 myotubes. *Febs J. 277*, 2180–2191.

(60) Coletti, D., Yang, E., Marazzi, G., and Sassoon, D. (2002) TNFα inhibits skeletal myogenesis through a PW1-dependent pathway by recruitment of caspase pathways. *EMBO J. 21*, 631–642.

(61) Zhao, Q., Yang, S. T., Wang, J. J., Zhou, J., Xing, S. S., Shen, C. C., Wang, X. X., Yue, Y. X., Song, J., Chen, M., Wei, Y. Y., Zhou, Q. P., Dai, T., and Song, Y. H. (2015) TNF alpha inhibits myogenic differentiation of C2C12 cells through NF-

κB activation and impairment of IGF-1 signaling pathway. *Biochem. Biophys. Res. Commun. 458*, 790–795.

(62) Yang, L., Nasu, Y., Hattori, M., Yoshimura, H., Kanno, A., and Ozawa, T. (2013) Bioluminescent probes to analyze ligand-induced phosphatidylinositol 3,4,5-trisphosphate production with split luciferase complementation. *Anal. Chem. 85*, 11352–11359.

(63) Miles, R. R., Perry, W., Haas, J. V, Mosior, M. K., Cho, M. N., Wang, J. W. J., Yu, P., Calley, J., Yue, Y., Carter, Q., Han, B., Foxworthy, P., Kowala, M. C., Ryan, T. P., Solenberg, P. J., and Michael, L. F. (2013) Genome-wide screen for modulation of hepatic apolipoprotien A-I(ApoA-I) secretion. *J. Biol. Chem. 288*, 6386–6396.

(64) Siles, S. A., Srinivasan, A., Pierce, C. G., Lopez-Ribot, J. L., and Ramasubramanian, A. K. (2013) High-throughput screening of a collection of known pharmacologically active small compounds for identification of Candida albicans biofilm inhibitors. *Antimicrob. Agents Chemother. 57*, 3681–3687.

(65) Waller, C. F. (2014) Imatinib mesylate. *Recent Results Cancer Res. 201*, 1–25.

(66) Hantschel, O., Rix, U., and Superti-Furga, G. (2008) Target spectrum of the BCR-ABL inhibitors imatinib, nilotinib and dasatinib. *Leuk. Lymphoma 49*, 615–619.

(67) Moryoussef, F., Dhooge, M., Volet, J., Barbe, C., Brezault, C., Hoeffel, C., Coriat, R., and Bouché, O. (2015) Reversible sarcopenia in patients with gastrointestinal stromal tumor treated with imatinib. *J. Cachexia. Sarcopenia Muscle 6*, 343–350.

(68) Parmar, S., Katsoulidis, E., Verma, A., Li, Y., Sassano, A., Lal, L., Majchrzak, B., Ravandi, F., Tallman, M. S., Fish, E. N., and Platanias, L. C. (2004) Role of the p38 Mitogen-activated Protein Kinase Pathway in the Generation of the Effects

of Imatinib Mesylate ( STI571 ) in BCR-ABL-expressing Cells. *J. Biol. Chem. 279*, 25345–25352.

(69) Perdiguero, E., Ruiz-Bonilla, V., Gresh, L., Hui, L., Ballestar, E., Sousa-victor, P., Baeza-raja, B., Esteller, M., Serrano, A. L., and Erwin, F. (2007) Genetic analysis of p38 MAP kinases in myogenesis: fundamental role of p38α in abrogating myoblast proliferation. *EMBO J. 26*, 1245–1256.

(70) Wu, Z., Woodring, P. J., Bhakta, K. S., Tamura, K., Wen, F., Feramisco, J. R., Karin, M., Wang, J. Y. J., and Puri, P. L. (2000) p38 and Extracellular Signal-Regulated Kinases Regulate the Myogenic Program at Multiple Steps. *Mol. Cell. Biol. 20*, 3951–3964.

(71) Omo, G. D., Penno, G., Prato, S. Del, Pedrinelli, R., Omo, D., and Prato, D. (2007) Doxazosin in metabolically complicated hypertension. *Expert Rev Cardiovasc Ther. 5*, 1027–1035.

(72) Boesch, S. T., Corvin, S., Zhang, J., Rogatsch, H., Bartsch, G., and Klocker, H. (1999) Modulation of the Differentiation Status of Cultured Prostatic Smooth Muscle Cells by an α1-Adrenergic Receptor Antagonist. *Prostate 39*, 226–233.

(73) Ogle, B. M., Cascalho, M., and Platt ||, J. L. (2005) Biological implications of cell fusion. *Nat. Rev. | Mol. CELL Biol. 6*, 567–575.

(74) Hernadez, J. M., and Podbilewicz, B. (2017) The hallmarks of cell-cell fusion. *Development 144*, 4481–4495.

(75) Bastida-Ruiz, D., Hoesen, K. Van, and Cohen, M. (2016) The dark side of cell fusion. *Int. J. Mol. Sci. 17*, 638.

## Acknowledgements

My deepest gratitude goes first and foremost to Prof. Takeaki Ozawa, my supervisor, for his constant encouragement and guidance. He has walked me through all the stages of the study and writing of this thesis. Without his consistent and illuminating instruction, this thesis could not have reached its present form.

Secondly, I would like to thank Prof. Hideaki Yoshimura who offered discussions and instructions on my experiments, Prof. Motonari Uesugi and Mr. Ken Tajiri who provided the chemical library and giving kind advices on the library selection, and Prof. Yutaka Hata who gave me instructions on the techniques for handling C212 cells.

Next, I would like to thank all committee members: Prof. Mitsuhiko Shionoya, Prof. Hiroshi Nishihara, Prof. Hiroaki Suga and Prof. Yuki Goto, for their patient readings of this dissertation and insightful advices on it.

I am also greatly indebted to express my heartfelt gratitude to Prof. Rintaro Shimada, Prof. Liangda Chiu, Dr. Natsumi Noda, Dr. Osamu Takenouchi and Dr. Maki Komiya, who kindly offers discussions on my experiments.

Although I have not listed them one by one, I also owe my sincere gratitude to all other members of Ozawa lab and my friends, who gave me their help and time in listening to me and helping me work out my problems during the difficult course of the thesis.

Last my thanks would go to my beloved family for their loving considerations and great confidence in me all through these years.